arXiv:2206.08134v2 [math.AP] 13 Sep 2022

Simple shear in nonlinear Cosserat micropolar elasticity: Existence of minimizers, numerical simulations and occurrence of microstructure

Thomas Blesgen*

Bingen University of Applied Sciences, Berlinstraße 109, D-55411 Bingen, Germany

Patrizio Neff

University of Duisburg-Essen, Faculty of Mathematics, Thea-Leymann-Straße 9, D-45127 Essen, Germany

Abstract

Deformation microstructure is studied for a $1D$-shear problem in geometrically nonlinear Cosserat elasticity. Microstructure solutions are described analytically and numerically for zero characteristic length scale.

Key words: Cosserat theory, microstructure, calculus of variations, micropolar, generalized continuum

Revised version.

1. Introduction

This article studies the formation of microstructure due to simple shear boundary conditions within a geometrically nonlinear Cosserat theory.

The Cosserat model is one of the best-known generalized continuum models [11]. It assumes that material points can undergo translation, described by the standard deformation map $\varphi : \Omega \to \mathbb{R}^3$ and independent rotations described by the orthogonal tensor field $R : \Omega \to \mathrm{SO}(3)$, where $\Omega \subset \mathbb{R}^3$ describes the reference configuration of the material. Therefore, the geometrically nonlinear Cosserat model induces immediately the Lie-group structure on the configuration space $\mathbb{R}^3 \times \mathrm{SO}(3)$.

*Corresponding author

URL: t.blesgen@th-bingen.de (Thomas Blesgen), patrizio.neff@uni-due.de (Patrizio Neff)

Both fields are coupled in the assumed elastic energy $W = W(\mathrm{D}\varphi, R, \mathrm{D}R)$ and the static Cosserat model appears as a two-field minimization problem which is automatically geometrically nonlinear due to the presence of the non-abelian rotation group SO(3). Material frame-indifference (objectivity) dictates left-invariance of the Lagrangian W under the action of SO(3) and material symmetry (here isotropy) implies right-invariance under action of SO(3).

In the early 20th century the Cosserat brothers E. and F. Cosserat introduced this model in its full geometrically nonlinear splendor [12] in a bold attempt to unify field theories embracing mechanics, optics and electrodynamics through a common principal of least action. They used the invariance of the energy under Euclidean transformations [13] to deduce the correct form of the energy $W = W(R^T\mathrm{D}\varphi, R^T\partial_x R, R^T\partial_y R, R^T\partial_z R)$ and to derive the equations of balance of forces (variations w.r.t. the deformation φ, the force-stress tensor may loose symmetry, [29]), and balance of angular momentum (variations w.r.t. rotations R). The Cosserat brothers did not provide, however, any specific constitutive form of the energy since they were not interested in specific applications.

1.1. Three-dimensional geometrically nonlinear isotropic Cosserat model

The underlying three-dimensional isotropic Cosserat model can be described in terms of the standard deformation mapping $\varphi : \Omega \subset \mathbb{R}^3 \to \mathbb{R}^3$ and an additional orthogonal microrotation tensor $R : \Omega \subset \mathbb{R}^3 \to \mathrm{SO}(3)$.

The goal here is to find a minimizer of the following isotropic energy[1]

$$\begin{aligned} E(\varphi, R) &= \int_\Omega \mu\big|\mathrm{sym}(\overline{U} - \mathbb{1}_3)\big|^2 + \mu_c\big|\mathrm{skew}(\overline{U} - \mathbb{1}_3)\big|^2 + \frac{\lambda}{4}\big((\det \overline{U} - 1)^2 + (\frac{1}{\det \overline{U}} - 1)^2\big) \\ &\qquad + \mu\frac{L_c^2}{2}\Big(a_1\big|\mathrm{dev\,sym}\, R^T\mathrm{Curl}R\,\big|^2 + a_2\big|\mathrm{skew}R^T\mathrm{Curl}R\big|^2 + \frac{a_3}{3}\mathrm{tr}(R^T\mathrm{Curl}R)^2\Big)\,\mathrm{dx} \\ &= \int_\Omega W_{\mathrm{mp}}(\overline{U}) + W_{\mathrm{disloc}}(R^T\mathrm{Curl}R)\,\mathrm{dx} \to \min \quad \text{w.r.t.} \quad (\varphi, R)\,, \qquad \overline{U} = R^T\mathrm{D}\varphi\,. \quad (1) \end{aligned}$$

The problem will be supplemented by Dirichlet boundary conditions for the deformation φ and the microrotations R can either be left free or prescribed or connected to $\mathrm{D}\varphi$ via the coupling condition $\mathrm{skew}(\overline{U})|_\Gamma = 0$ with $\Gamma = \partial\Omega$. Here, $\mu > 0$ is the standard elastic shear modulus, λ the second elastic Lamé parameter and $\mu_c \geq 0$ is the so-called Cosserat couple modulus; a_1, a_2, a_3 are non-dimensional non-negative weights and $L_c > 0$ is a characteristic length. The isotropic energy (1) is written in terms of the nonsymmetric Biot type stretch tensor $\overline{U} = R^T\mathrm{D}\varphi$ (first Cosserat deformation tensor, [12]) and the curvature measure $R^T\mathrm{Curl}R$. We call $\alpha := R^T\mathrm{Curl}R$

[1]The volumetric term $\frac{\lambda}{4}\big((\det \overline{U} - 1)^2 + (\frac{1}{\det \overline{U}} - 1)^2\big)$ is independent of the microrotation R and polyconvex in $\mathrm{D}\varphi$. It's quadratic approximation is $\frac{\lambda}{2}\mathrm{tr}^2(\overline{U} - \mathbb{1}_3)$.

the *second order* dislocation density tensor, [4]. Due to the orthogonality of dev sym, skew and tr(.)$\mathbb{1}$, the curvature energy provides a complete control of

$$|\alpha|^2 = \left|R^T \mathrm{Curl} R\right|^2 = |\mathrm{Curl} R|^2 \qquad \text{provided} \qquad a_1, a_2, a_3 > 0\,. \tag{2}$$

Using the result in [30],

$$\left|\mathrm{Curl} R\,\right|^2_{\mathbb{R}^{3\times 3}} \geq c^+ |\mathrm{D}R\,|^2_{\mathbb{R}^{3\times 3\times 3}}\,, \tag{3}$$

shows that the energy (1) controls DR in $L^2(\Omega, \mathbb{R}^{3\times 3\times 3})$.

In this setting, the minimization problem is highly non-convex w.r.t. (φ, R). Existence of minimizers for (1) with $\mu_c > 0$ has been shown first in [25], see also [26, 25, 21, 4, 23], the partial regularity for minimizers of a related problem is investigated in [22, 19]. The Cosserat couple modulus μ_c controls the deviation of the microrotation R from the continuum rotation polar(Dφ) in the polar decomposition of Dφ = polar(Dφ) $\cdot \sqrt{\mathrm{D}\varphi^T \mathrm{D}\varphi}$, cf. [27].

For $\mu_c \to \infty$ the constraint R = polar(Dφ) is generated and the model would turn into a Toupin couple stress model.

Here we derive the three-dimensional Euler-Lagrange equations based on the curvature expressed in the dislocation tensor $\alpha = R^T \mathrm{Curl} R$. We can write the bulk elastic energy as

$$E(\varphi, R) = \int_\Omega W_{\mathrm{mp}}(\overline{U}) + W_{\mathrm{disloc}}(\alpha)\ \mathrm{dx}\,, \qquad \overline{U} = R^T \mathrm{D}\varphi\,, \qquad \alpha = R^T \mathrm{Curl} R\,. \tag{4}$$

Taking variations of (4) w.r.t. the deformation φ leads to

$$\begin{aligned} \delta E(\varphi, R)\cdot\delta\varphi &= \int_\Omega \langle \mathrm{D}W_{\mathrm{mp}}(\overline{U}), R^T \mathrm{D}\delta\varphi\rangle_{\mathbb{R}^{3\times 3}}\ \mathrm{dx} = 0\,, \qquad \forall\ \delta\varphi \in C_0^\infty(\Omega, \mathbb{R}^3) \\ &\iff \int_\Omega \langle R\,\mathrm{D}W_{\mathrm{mp}}(\overline{U}), \mathrm{D}\delta\varphi\rangle_{\mathbb{R}^{3\times 3}}\ \mathrm{dx} = \int_\Omega \langle \mathrm{Div}[R\cdot \mathrm{D}W_{\mathrm{mp}}(\overline{U})], \delta\varphi\rangle_{\mathbb{R}^3}\ \mathrm{dx} = 0\,. \end{aligned} \tag{5}$$

Taking variation w.r.t. $R \in \mathrm{SO}(3)$ results in (abbreviate $F := \mathrm{D}\varphi$)

$$\begin{aligned} \delta E(\varphi, R)\cdot\delta R &= \int_\Omega \langle \mathrm{D}W_{\mathrm{mp}}(\overline{U}), \delta R^T F\rangle + \langle \mathrm{D}W_{\mathrm{disloc}}(\alpha), \delta R^T \mathrm{Curl} R + R^T \mathrm{Curl}\delta R\rangle\ \mathrm{dx} \\ &= \int_\Omega \langle \mathrm{D}W_{\mathrm{mp}}(\overline{U}), \delta R^T R\cdot R^T F\rangle + \langle \mathrm{D}W_{\mathrm{disloc}}(\alpha), \delta R^T R\cdot R^T \mathrm{Curl} R + R^T \mathrm{Curl}\delta R\rangle\ \mathrm{dx} \\ &= \int_\Omega \langle \mathrm{D}W_{\mathrm{mp}}(\overline{U})\cdot \overline{U}^T, \delta R^T R\rangle + \langle \mathrm{D}W_{\mathrm{disloc}}(\alpha), \delta R^T R\cdot \alpha + R^T \mathrm{Curl}\delta R\rangle\ \mathrm{dx} = 0\,. \end{aligned} \tag{6}$$

Since $R^T R = \mathbb{1}$, it follows that $\delta R^T R + R^T \delta R = 0$ and $\delta R^T R = A \in \mathfrak{so}(3)$ is arbitrary. Therefore, Eqn. (6) can be written as

$$0 = \int_\Omega \langle \mathrm{D}W_{\mathrm{mp}}(\overline{U})\cdot \overline{U}^T, A\rangle + \langle \mathrm{D}W_{\mathrm{disloc}}(\alpha)\cdot \alpha^T, A\rangle + \langle \mathrm{D}W_{\mathrm{disloc}}(\alpha), R^T \mathrm{Curl}(RA^T)\rangle\ \mathrm{dx} \tag{7}$$

for all $A \in C_0^\infty(\Omega, \mathfrak{so}(3))$. Using that Curl is a self-adjoint operator, this is equal to

$$0 = \int_\Omega \langle \mathrm{D}W_{\mathrm{mp}}(\overline{U}) \cdot \overline{U}^T + \mathrm{D}W_{\mathrm{disloc}}(\alpha)\, \alpha^T, A\rangle + \langle \mathrm{Curl}(R\, \mathrm{D}W_{\mathrm{disloc}}(\alpha)), RA^T\rangle \,\mathrm{dx} \tag{8}$$
$$= \int_\Omega \langle \mathrm{D}W_{\mathrm{mp}}(\overline{U}) \cdot \overline{U} + \mathrm{D}W_{\mathrm{disloc}}(\alpha)\, \alpha^T - R^T \mathrm{Curl}(R\, \mathrm{D}W_{\mathrm{disloc}}(\alpha)), A\rangle \,\mathrm{dx} \qquad \forall A \in C_0^\infty(\Omega, \mathfrak{so}(3))\,.$$

Thus, the strong form of the Euler-Lagrange equations reads

$$\begin{aligned} \mathrm{Div}[R\, \mathrm{D}W_{\mathrm{mp}}(\overline{U})] &= 0\,, && \text{"balance of forces"}\,, \\ \mathrm{skew}[R^T\, \mathrm{Curl}(R\, \mathrm{D}W_{\mathrm{disloc}}(\alpha))] &= \mathrm{skew}(\mathrm{D}W_{\mathrm{mp}}(\overline{U}) \cdot \overline{U}^T + \mathrm{D}W_{\mathrm{disloc}}(\alpha) \cdot \alpha^T)\,, \\ & && \text{"balance of angular momentum"}\,. \end{aligned} \tag{9}$$

If $\mathrm{D}W_{\mathrm{disloc}}(\alpha) \equiv 0$ (no moment stresses, zero characteristic length $L_c = 0$) then balance of angular momentum turns into the symmetry constraint

$$\mathrm{D}W_{\mathrm{mp}}(\overline{U}) \cdot \overline{U}^T \in \mathrm{Sym}(3)\,. \tag{10}$$

A complete discussion of the solutions [18] to this constraint and applications can be found in [9, 28, 29, 3].

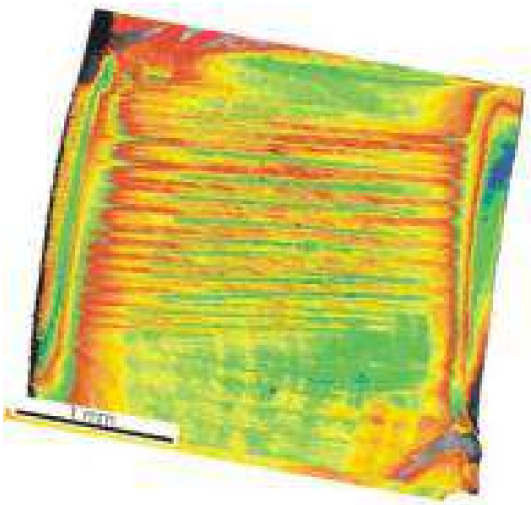


Figure 1: A single crystal copper specimen in simple shear, showing glide planes and micro bands. Lattice rotations do not coincide with continuum rotations. Courtesy of D. Raabe, MPI-Eisenforschung, Düsseldorf [16].

2. The Cosserat model in simple shear

In order to elucidate the proposed nonlinear theory, notably the impact of boundary and side conditions on the microrotations, we consider the deformation of an infinite layer of material with unit height, fixed at the bottom and sheared in e_1-direction with amount γ at the upper face. We impose the boundary conditions $\varphi(x_1, x_2, 0) = (x_1, x_2, 0)^T$, $\varphi(x_1, x_2, 1) = (x_1 + \gamma, x_2, x_3)^T$, $x_1, x_2 \in \mathbb{R}$. The parameter $\gamma \geq 0$ is the amount of maximal shear at the upper face per unit length. The most general deformations are of the form

$$\varphi(x_1, x_2, x_3) = (x_1 + u(x_1, x_2), x_2, x_3 + v(x_1, x_3))^T,$$

see Fig 2. Hence, we look for energy minimizing deformations in the form

$$\varphi(x_1, x_2, x_3) = \begin{pmatrix} x_1 + u(x_1, x_3) \\ x_2 \\ x_3 + v(x_1, x_3) \end{pmatrix}, \quad \mathrm{D}\varphi(x_1, x_2, x_3) = \begin{pmatrix} 1 + u_{x_1}(x_1, x_3) & 0 & u_{x_3}(x_1, x_3) \\ 0 & 1 & 0 \\ v_{x_1}(x_1, x_3) & 0 & 1 + v_{x_3}(x_1, x_3) \end{pmatrix}, \tag{11}$$

with $u(x_1, 0) = 0, u(x_1, 1) = \gamma$. The infinite extension in e_1-direction implies that ∂_{x_1} must vanish and from symmetry of the boundary conditions at the upper and lower face, there is no reason for a displacement in e_3-direction either. Hence the reduced kinematics

$$\varphi(x_1, x_2, x_3) = \begin{pmatrix} x_1 + u(x_3) \\ x_2 \\ x_3 \end{pmatrix}, \quad F = \mathrm{D}\varphi(x_1, x_2, x_3) = \begin{pmatrix} 1 & 0 & u'(x_3) \\ 0 & 1 & 0 \\ 0 & 0 & 1 \end{pmatrix}, \tag{12}$$

with $u(0) = 0$, $u(1) = \gamma$ suffices. The considered problem is therefore the exact formulation of the simple shear in e_1-direction with amount γ at the upper face of a layer of material with unit height, fixed at the bottom.

Accordingly, we assume microrotations $R \in \mathrm{SO}(3)$ in the form

$$R(x_1, x_2, x_3) = \begin{pmatrix} \cos\alpha(x_3) & 0 & \sin\alpha(x_3) \\ 0 & 1 & 0 \\ -\sin\alpha(x_3) & 0 & \cos\alpha(x_3) \end{pmatrix}, \tag{13}$$

having fixed axis of rotation e_2. Therefore,

$$\mathrm{Curl} R = \begin{pmatrix} 0 & -\sin\alpha(x_3)\alpha'(x_3) & 0 \\ 0 & 0 & 0 \\ 0 & -\cos\alpha(x_3)\alpha'(x_3) & 0 \end{pmatrix}. \tag{14}$$

In the following, we denote x_3 by x. It holds $|\overline{R}^T \mathrm{Curl}\overline{R}|^2 = |\mathrm{Curl}\overline{R}|^2 = |\overline{\alpha}'|^2$.

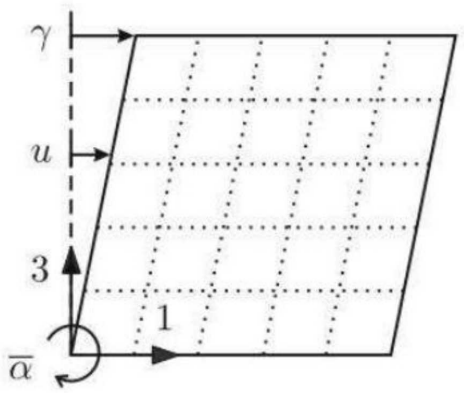


Figure 2: The deformed state exhibits a homogeneous region in the interior of the structure which motivates the kinematics of simple shear.

Inserting the ansatz (11) and (13) leaves us with the energy

$$\begin{aligned} E(u,\alpha) &= \int_0^1 W(u',\alpha,\alpha')\,\mathrm{dx} \\ &:= \mu\int_0^1 2L_c^2|\alpha'|^2+2(\cos(\alpha)-1)^2+\frac{1+\sin^2(\alpha)}{2}|u'|^2+2(\cos(\alpha)-1)\sin(\alpha)u'\,\mathrm{dx} \\ &\quad + \frac{\mu_c}{2}\int_0^1 \cos^2(\alpha)\big(2\tan(\alpha)-u'\big)^2\,\mathrm{dx}. \end{aligned} \tag{15}$$

3. A one-dimensional simple shear problem

In this article we are now concerned with minimizers of the *mechanical energy functional*

$$\begin{aligned} E(u,\alpha) &= \mu\int_0^1 2L_c^2|\alpha'|^2+2(\cos(\alpha)-1)^2+\frac{1+\sin^2(\alpha)}{2}|u'|^2+2(\cos(\alpha)-1)\sin(\alpha)u'\,\mathrm{dx} \\ &\quad + \frac{\mu_c}{2}\int_0^1 \cos^2(\alpha)\big(2\tan(\alpha)-u'\big)^2\,\mathrm{dx}. \end{aligned} \tag{16}$$

Introducing the third-order expansion $\cos(\alpha)\sim 1-\frac{\alpha^2}{2}$, $\sin(\alpha)\sim\alpha-\frac{\alpha^3}{6}$ and dropping the higher order terms leads to the *reduced mechanical energy functional*

$$\begin{aligned} E_{\mathrm{red}}(u,\alpha) &:= \mu\int_0^1 \Big(2L_c^2|\alpha'|^2+\frac{1+\alpha^2}{2}|u'|^2+\frac{\alpha^4}{2}-\alpha^3u'\Big)\,\mathrm{dx} \\ &\quad + 2\mu_c\int_0^1 \Big(\frac{u'}{2}-\alpha\Big)\Big(\frac{u'}{2}-\alpha-\frac{\alpha^2}{6}(3u'-2\alpha)\Big)\,\mathrm{dx}. \end{aligned} \tag{17}$$

For the definitions (16) and (17), see also [31][Eqn.(3.11), Eqn.(3.22)]. We first provide alternative representations of these two functionals as this allows to simplify the Euler-Lagrange equations and will give insights into the minimizers later.

Lemma 1. *The functionals E, $E_{\rm red}$ defined in (16), (17) can alternatively be written as*

$$\begin{aligned} E(u,\alpha) &= \int_0^1 W(u',\alpha,\alpha')\,\mathrm{dx} \qquad (18)\\ &= \frac{\mu}{2}\int_0^1 4L_c^2|\alpha'|^2+|u'|^2+\Big(\sin(\alpha)u'-4\sin^2\big(\frac{\alpha}{2}\big)\Big)^2\,\mathrm{dx}\\ &\quad+\frac{\mu_c}{2}\int_0^1\Big(\cos(\alpha)u'-2\sin(\alpha)\Big)^2\,\mathrm{dx}, \qquad (19)\end{aligned}$$

$$\begin{aligned} E_{\rm red}(u,\alpha) &= \frac{\mu}{2}\int_0^1 4L_c^2|\alpha'|^2+|u'|^2+[\alpha(\alpha-u')]^2\,\mathrm{dx}\\ &\quad+\frac{\mu_c}{2}\int_0^1(1-\alpha^2)|u'|^2+\Big(\frac{8\alpha^2}{3}-4\Big)\alpha u'+4\alpha^2-\frac{4\alpha^4}{3}\,\mathrm{dx}. \qquad (20)\end{aligned}$$

Proof. Both identities follow from straightforward elementary rearrangements. Trigonometric addition formulas imply $\cos(2\alpha)=\cos^2(\alpha)-\sin^2(\alpha)=1-2\sin^2(\alpha)$, hence

$$\cos(\alpha)-1=-2\sin^2\big(\frac{\alpha}{2}\big). \qquad (21)$$

Plugging (21) into (16) yields

$$\begin{aligned} &2(\cos(\alpha)-1)^2+\frac{1+\sin^2(\alpha)}{2}|u'|^2+2(\cos(\alpha)-1)\sin(\alpha)\,u'\\ &\quad=\ 8\sin^4\big(\frac{\alpha}{2}\big)+\frac{|u'|^2}{2}+\frac{\sin^2(\alpha)|u'|^2}{2}-4u'\sin^2\big(\frac{\alpha}{2}\big)\sin(\alpha)\\ &\quad=\ \frac{1}{2}\Big(\sin(\alpha)u'-4\sin^2\big(\frac{\alpha}{2}\big)\Big)^2+\frac{|u'|^2}{2}. \qquad (22)\end{aligned}$$

Similarly, for the μ_c-integral in (16),

$$\begin{aligned} &\cos^2(\alpha)(2\tan(\alpha)-u')^2=\cos^2(\alpha)\big(4\tan^2(\alpha)-4\tan(\alpha)u'+|u'|^2\big)\\ &\quad=\ 4\sin^2(\alpha)-4\sin(\alpha)\cos(\alpha)u'+\cos^2(\alpha)|u'|^2=\Big(\cos(\alpha)u'-2\sin(\alpha)\Big)^2. \qquad (23)\end{aligned}$$

This proves (19). The proof of (20) is immediate from

$$\frac{1+\alpha^2}{2}|u'|^2+\frac{\alpha^4}{2}-\alpha^3u'=\frac{|u'|^2}{2}+\frac{\alpha^2}{2}\Big(|u'|^2-2\alpha u'+\alpha^2\Big),$$

and a re-ordering of the μ_c-integral. □

Remark 1. *The μ_c-part of $E_{\rm red}$ cannot be written as a complete quadratic form since some higher order terms have been dropped. However, by keeping the terms $\frac{\mu_c}{2}\Big(\frac{\alpha^4}{4}|u'|^2-\frac{1}{3}\alpha^5u'+\frac{1}{9}\alpha^6\Big)$ of the Taylor expansion of W, we find*

$$E_{\rm red}(u,\alpha) \;=\; \int_0^1 W_{\rm red}(u',\alpha,\alpha')\,{\rm dx} \tag{24}$$

$$\;=\; \frac{\mu}{2}\int_0^1 4L_c^2|\alpha'|^2+|u'|^2+[\alpha(\alpha-u')]^2\,{\rm dx}+\frac{\mu_c}{2}\int_0^1\Big(\frac{2-\alpha^2}{2}u'-\frac{6\alpha-\alpha^3}{3}\Big)^2\,{\rm dx}. \tag{25}$$

From now on we will use this representation (25) instead of (20).

We consider the minimization problem

$$E(u,\alpha)\to\min \tag{26}$$

subject either to the *consistent coupling conditions* [15] (derived from ${\rm skew}(R^TF)_{|\{0,1\}}=0$)

$$u(0)=0,\ u(1)=\gamma, \qquad\qquad u'(0)=2\tan(\alpha(0)),\quad u'(1)=2\tan(\alpha(1)) \tag{27}$$

or subject to the *Dirichlet boundary conditions* (for prescribed microrotation angle $\alpha_D\in\mathbb{R}$ at the upper and lower faces)

$$u(0)=0,\ u(1)=\gamma, \qquad\qquad \alpha(0)=\alpha(1)=\alpha_D. \tag{28}$$

In order to single out solutions, we may impose the further *symmetry constraint*

$$u'(1)=u'(0). \tag{29}$$

The Euler-Lagrange equations related to (26), replacing [31][Eqn. (3.14)], read

$$[2\mu+(\mu_c-\mu)\cos^2(\alpha)]u'' \;=\; 2(\mu_c-\mu)\Big(\sin(\alpha)\cos(\alpha)u'+\cos^2(\alpha)-\sin^2(\alpha)\Big)\alpha'+2\mu\cos(\alpha)\alpha', \tag{30}$$

$$4\mu L_c^2\alpha'' \;=\; \big(\cos(\alpha)u'-2\sin(\alpha)\big)\big[(\mu-\mu_c)\big(\sin(\alpha)u'-4\sin^2\big(\frac{\alpha}{2}\big)\big)-2\mu_c\big] \tag{31}$$

for $x=x_3\in\Omega:=(0,1)$ subject to either (27), (29) or (28), (29). The equations (30), (31) constitute balance of force and angular momentum, respectively. Eqn. (31) is the form that Eqn. (10) takes for the ansatz made here.

Eqn. (30) is equivalent to $\frac{\rm d}{\rm dx}\tau(u,\alpha)=0$ in Ω for the *force stress tensor* $\tau=\tau(u,\alpha)$ defined by

$$\tau:={\rm D}_{u'}W(u',\alpha,\alpha')=\mu\Big[u'+\sin(\alpha)\Big(\sin(\alpha)u'-4\sin^2\big(\frac{\alpha}{2}\big)\Big)\Big]+\mu_c\cos(\alpha)\Big[\cos(\alpha)u'-2\sin(\alpha)\Big]. \tag{32}$$

The Euler-Lagrange equations related to $E_{\rm red}(u,\alpha) \to \min$ lead to the *reduced system*

$$-\Big[\mu(1+\alpha^2)+\mu_c\Big(1-\alpha^2+\underline{\frac{1}{4}\alpha^4}\Big)\Big]u'' = (4\mu_c-3\mu)\alpha^2\alpha' + 2(\mu-\mu_c)\alpha\alpha'\,u' - 2\mu_c\alpha' \\ \underline{+\mu_c\alpha^3\Big(u'-\frac{5}{6}\alpha\Big)\alpha'}, \tag{33}$$

$$\mu\Big(-L_c^2\alpha'' + \frac{1}{2}\alpha^3 - \frac{3}{4}\alpha^2u' + \frac{1}{4}\alpha|u'|^2\Big) + \mu_c\Big(-\frac{1}{4}\alpha|u'|^2 + \alpha^2u' - \frac{2}{3}\alpha^3 + \alpha - \frac{1}{2}u'\Big) \\ \underline{+\mu_c\Big(\frac{1}{8}\alpha^3|u'|^2 - \frac{5}{24}\alpha^4u' + \frac{1}{12}\alpha^5\Big)} = 0 \tag{34}$$

for $x = x_3 \in \Omega := (0,1)$ subject either to the reduced consistent coupling boundary conditions

$$u(0) = 0,\ u(1) = \gamma, \qquad\qquad 2\alpha(0) = u'(0),\ 2\alpha(1) = u'(1) \tag{35}$$

and (29) or subject to (28) and (29). Underlined in (33), (34) are those higher order terms that are only present if $E_{\rm red}$ is defined by (25) instead of (17) or (20).
Eqn. (33) is equivalent to $\frac{\rm d}{\rm dx}\tau_{\rm red}(u,\alpha) = 0$ in Ω for the *reduced force stress tensor* $\tau_{\rm red} = \tau_{\rm red}(u,\alpha)$ defined by

$$\tau_{\rm red} := {\rm D}_{u'}W(u',\alpha,\alpha') = \mu\Big[u' - \alpha^2(\alpha-u')\Big] + \mu_c\Big(\frac{2-\alpha^2}{2}\Big)\Big[\frac{2-\alpha^2}{2}u' - \frac{6\alpha-\alpha^3}{3}\Big]. \tag{36}$$

We point out that Eqn. (34) can equally be written as

$$\mu L_c^2\alpha'' = \mu\,\partial_\alpha\Phi_u(\alpha) + \mu_c\,\partial_\alpha Q_u(\alpha) \tag{37}$$

with the potentials

$$\Phi_u(\alpha) := \frac{1}{8}\alpha^2(\alpha-u')^2, \qquad\qquad Q_u(\alpha) := \frac{1}{8}\Big(\frac{2-\alpha^2}{2}u' - \frac{6\alpha-\alpha^3}{3}\Big)^2. \tag{38}$$

For small values $\mu_c \geq 0$, the double-well potential Φ_u is dominant and Eqn. (37) corresponds to a stationary Allen-Cahn equation[2]. The larger the Cosserat couple modulus μ_c, the stronger the influence of the quadratic potential Q_u. There is a bifurcation and a critical value $\mu_c^{\rm crit}$, such that for $\mu_c \geq \mu_c^{\rm crit}$, the right hand side of Eqn. (37) has only one minimizer, see Figs. 3.

Related to different boundary conditions we introduce the reflexive Banach spaces

$$\mathcal{X}^D := \Big\{(u,\alpha)\in(W^{1,2}(\Omega;\,\mathbb{R}))^2 \,\Big|\, u(0)=0,\ u(1)=\gamma, \quad \alpha(0)=\alpha(1)=\alpha_D\Big\}, \\ X^D := \Big\{(u,\alpha)\in W^{1,2}(\Omega;\,\mathbb{R})\times L^4(\Omega;\,\mathbb{R}) \,\Big|\, u(0)=0,\ u(1)=\gamma, \quad \alpha(0)=\alpha(1)=\alpha_D\Big\} \tag{39}$$

[2]Allen-Cahn equation: $\partial_t u = \varepsilon\Delta u - \psi'(u)$ with a double-well potential ψ.

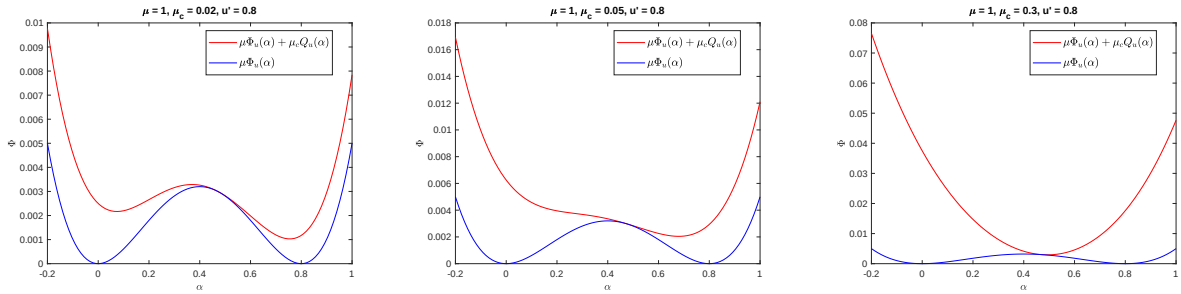


Figure 3: The potential $\mu\,\Phi_u(\alpha) + \mu_c\,Q_u(\alpha)$ (in red) compared to the double-well potential $\mu\,\Phi_u(\alpha)$ (in blue) for $\alpha \in [-0.2, 1]$, $u' = 0.8$ and $\mu = 1$. Left: $\mu_c = 0.02$. Center: $\mu_c = 0.05$. Right: $\mu_c = 0.3$.

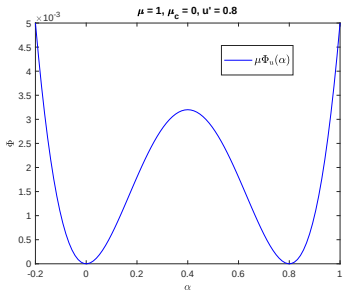


Figure 4: The double-well potential $\mu\Phi_u(\alpha)$ for $\alpha \in [-0.2, 1]$, $u' = 0.8$ and $\mu = 1$.

and correspondingly for the consistent coupling conditions

$$\begin{aligned}
\mathcal{X}^C_{\text{red}} &:= \Big\{(u,\alpha) \in (W^{1,2}(\Omega;\,\mathbb{R}))^2 \,\Big|\, u(0) = 0,\; u(1) = \gamma,\; 2\alpha(0) = u'(0),\; 2\alpha(1) = u'(1)\Big\},\\
\mathcal{X}^C &:= \Big\{(u,\alpha) \in (W^{1,2}(\Omega;\,\mathbb{R}))^2 \,\Big|\, u(0) = 0,\; u(1) = \gamma,\; 2\tan\alpha(0) = u'(0),\; 2\tan\alpha(1) = u'(1)\Big\}, \quad (40)\\
X^C_{\text{red}} &:= \Big\{(u,\alpha) \in W^{1,2}(\Omega;\,\mathbb{R}) \times L^4(\Omega;\,\mathbb{R}) \,\Big|\, u(0) = 0,\; u(1) = \gamma,\; 2\alpha(0) = u'(0),\; 2\alpha(1) = u'(1)\Big\},\\
X^C &:= \Big\{(u,\alpha) \in W^{1,2}(\Omega;\,\mathbb{R}) \times L^4(\Omega;\,\mathbb{R}) \,\Big|\, u(0) = 0,\; u(1) = \gamma,\; 2\tan\alpha(0) = u'(0), 2\tan\alpha(1) = u'(1)\Big\}.
\end{aligned}$$

Lemma 2. *Let $L_c > 0$. Then, for any $\mu > 0$, $\mu_c \geq 0$, E_{red} defined by (25) possesses a minimizer (u,α) in $\mathcal{X}^C_{\text{red}}$, $\mathcal{X}^D$ and E possesses a minimizer in $\mathcal{X}^C$, $\mathcal{X}^D$. For $L_c = 0$, E_{red} has minimizers in X^C_{red}, X^D and E has minimizers in X^C, X^D.*

Proof. (i) Let $L_c > 0$. We first consider the case of Dirichlet boundary conditions for u and α. Rewriting (25) as a functional defined on $\mathcal{X}_0 := (W^{1,2}_0((0,1);\,\mathbb{R})^2$, we find with Young's

inequality for $(u,\alpha)\in\mathcal{X}_0$

$$\begin{aligned}
E_{\mathrm{red}}(u+\gamma,\alpha+\alpha_D) = {}& \frac{\mu}{2}\int_0^1 4L_c^2|\alpha'|^2+(u'+\gamma)^2+\big[(\alpha+\alpha_D)(\alpha+\alpha_D-(u'+\gamma))\big]^2\,\mathrm{dx}\\
&+\frac{\mu_c}{2}\int_0^1\Big(\frac{2-(\alpha+\alpha_D)^2}{2}(u'+\gamma)-\frac{6(\alpha+\alpha_D)-(\alpha+\alpha_D)^3}{3}\Big)^2\,\mathrm{dx}\\
\geq {}& \frac{\mu}{2}\int_0^1 4L_c^2|\alpha'|^2+(u'+\gamma)^2\,\mathrm{dx} \qquad (41)\\
= {}& \mu\int_0^1 2L_c^2|\alpha'|^2+\frac{1}{2}|u'|^2+\big(\frac{u'}{2}\big)(2\gamma)+\frac{\gamma^2}{2}\,\mathrm{dx}\\
\geq {}& \mu\int_0^1 2L_c^2|\alpha'|^2+\frac{1}{2}|u'|^2-\frac{1}{4}|u'|^2-4\gamma^2+\frac{\gamma^2}{2}\,\mathrm{dx}\\
= {}& \mu\int_0^1 2L_c|\alpha'|^2+\frac{1}{4}|u'|^2-\frac{7\gamma^2}{2}\,\mathrm{dx}.
\end{aligned}$$

With the Poincaré inequality valid on $\mathcal{X}_0$ and the Banach-Alaoglu theorem this demonstrates that the level sets

$$\Big\{(u,\alpha)\in\mathcal{X}^D\;\Big|\;E_{\mathrm{red}}(u,\alpha)\leq C\Big\}$$

for constants $C>0$ are sequentially weakly precompact proving the coercivity of E_{red}, see, e.g. [32].

We observe that the integrand $W_{\mathrm{red}}(u',\alpha,\alpha')$ as defined in (24) is a Carathéodory function and strictly convex both in u' and α'. Despite the dependence of W_{red} on α, the proof of weak lower semicontinuity of E_{red} in $\mathcal{X}^D$ can thus be carried out in the spirit of the well-known Tonelli-Serrin theorem, see [14, Section 3.2.6] for details. Alternatively, the weak lower semicontinuity can be derived from the more general result in [1] based on gradient Young measures. By the direct method in the calculus of variations, the coercivity and weak lower semicontinuity of E_{red} yield the existence of a minimizer $(u,\alpha)\in\mathcal{X}^D$. The proof of minimizers of E_{red} in $\mathcal{X}^C_{\mathrm{red}}$ is similar.

Now let us consider the case of Dirichlet boundary conditions for E. Proceeding as above and estimating the quadratic terms from below by 0, we find for $(u,\alpha)\in\mathcal{X}_0$

$$E(u+\gamma,\alpha+\alpha_D)\geq\frac{\mu}{2}\int_0^1 4L_c^2|\alpha'|^2+(u'+\gamma)^2\,\mathrm{dx}.$$

This coincides with (41). From there, with the Poincaré inequality the coercivity of E in $\mathcal{X}^D$ can be shown as above. The lower semicontinuity of E is again a consequence of strict convexity and the Tonelli-Serrin theorem. The proof of minimizers of E in $\mathcal{X}^C$ is similar.

(ii) Let $L_c=0$. The coercivity of E_{red} w.r.t. weak-convergence can be shown similar to (i). In contrast, E is 2π-periodic in α which replaces the coercivity in α. Eqns. (25), (19) imply the lower semicontinuity of E_{red}, E. With the direct method, the existence of minimizers of E_{red} in X^D, X^C_{red} and of E in X^D, X^C for any $\mu>0$, $\mu_c\geq 0$ follows. □

For the detailed discussion of the Euler-Lagrange equations related to problem (26) we introduce the function

$$\eta(\alpha) := \frac{4\sin^2\left(\frac{\alpha}{2}\right)}{\sin(\alpha)}. \tag{42}$$

It holds $\lim_{\alpha\to 0}\eta(\alpha) = 0$ and $\eta(\alpha)$ is invertible, monotone increasing and close to a linear function, cf. Fig. 5.

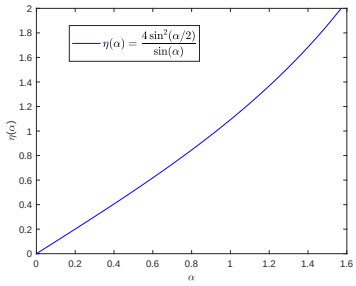


Figure 5: Plot of the function $\eta(\alpha) = \frac{4\sin^2\left(\frac{\alpha}{2}\right)}{\sin(\alpha)}$ for $\alpha \in \left[0, \frac{\pi}{2}\right]$.

In the following discussion, we first ignore the boundary conditions on u and α and study sufficiently regular solutions $u \in W^{2,2}(\Omega)$ and $\alpha \in W^{1,2}(\Omega)$. Clearly, not every solution is in this class, c.f. Section 4.

Lemma 3. *Let $L_c = 0$ and $\mu > 0$, $\mu_c \geq 0$. Then every solution*

$$(u, \alpha) \in W^{2,2}(\Omega) \times W^{1,2}(\Omega)$$

of the Euler-Lagrange equations (30), (31) is continuous in $\overline{\Omega}$ and satisfies

$$u''(x) = \alpha'(x) = 0 \text{ for a.e. } x \in \Omega. \tag{43}$$

Proof. Due to the Sobolev embedding $W^{1,2}(\Omega) \hookrightarrow C^0(\overline{\Omega})$, both α and u are continuous.

(i) For $\mu = \mu_c$, the Euler-Lagrange equations (30), (31) simplify to

$$u'' = \cos(\alpha)\alpha', \tag{44}$$

$$0 = \cos(\alpha)u' - 2\sin(\alpha) \tag{45}$$

to be satisfied pointwise for $x \in \Omega$.

Eqn. (45) is equivalent to $u' = 2\tan(\alpha)$ and taking the derivative yields $u'' = \frac{2\alpha'}{\cos^2(\alpha)}$. With (44) we find

$$\frac{2\alpha'}{\cos^2(\alpha)} = \cos(\alpha)\alpha'. \tag{46}$$

Since $2 = \cos^3(\alpha)$ has no solution, Eqn. (46) implies $\alpha' = 0$, and so with (44) $u'' = 0$.

(ii) Let $\mu > 0$, $\mu_c \geq 0$ with $\mu \neq \mu_c$. Considering the Euler-Lagrange equation (31) with $L_c = 0$, two cases may occur.

Case 1: $\alpha = \arctan\big(\frac{u'}{2}\big)$.

This implies $u' = 2\tan(\alpha)$ such that $u'' = \frac{2\alpha'}{\cos^2(\alpha)}$. Inserting this identity in (30) yields

$$(\mu_c - \mu)\frac{\big[\sin(\alpha)\cos(\alpha)u' + \cos^2(\alpha) - \sin^2(\alpha)\big]\alpha'}{2\mu + (\mu_c - \mu)\cos^2(\alpha)} + \frac{\mu\cos(\alpha)\alpha'}{2\mu + (\mu_c - \mu)\cos^2(\alpha)} = \frac{\alpha'}{\cos^2(\alpha)}. \tag{47}$$

[The denominator in (47) is positive, e.g. $2\mu + (\mu_c - \mu)\cos^2(\alpha) \geq 2\mu > 0$ for $\mu_c \geq \mu$ and $2\mu + (\mu_c - \mu)\cos^2(\alpha) \geq 2\mu - (\mu_c - \mu) > 0$ for $\mu_c < \mu$.]

Using $u' = 2\tan(\alpha)$ on the right gives after simplifications

$$\frac{\big[\mu_c - \mu + \mu\cos(\alpha)\big]\alpha'}{2\mu + (\mu_c - \mu)\cos^2(\alpha)} = \frac{\alpha'}{\cos^2(\alpha)} \tag{48}$$

which is equivalent to

$$\mu\cos^3(\alpha)\alpha' = 2\mu\alpha'.$$

Since $\mu > 0$, this proves as in (i) that $\alpha' = 0$ which with (30) results in $u'' = 0$.

Case 2: $\sin(\alpha)u' = 4\sin^2\big(\frac{\alpha}{2}\big) + \frac{2\mu_c}{\mu - \mu_c}$.

For $\mu_c = 0$, one solution is $\alpha \equiv 2\pi k$ for some $k \in \mathbb{Z}$. Then $\alpha' = 0$ and Eqn. (30) shows $u'' = 0$. Alternatively, for $\alpha \not\equiv 2\pi k$, we have $\sin(\alpha) \neq 0$ such that

$$u' = \frac{2\mu_c}{(\mu - \mu_c)\sin(\alpha)} + \frac{4\sin^2\big(\frac{\alpha}{2}\big)}{\sin(\alpha)}. \tag{49}$$

Taking the derivative yields

$$u'' = -\frac{2\mu_c\cos(\alpha)\alpha'}{(\mu - \mu_c)\sin^2(\alpha)} + \frac{\big[4\sin\big(\frac{\alpha}{2}\big)\cos\big(\frac{\alpha}{2}\big)\sin(\alpha) - 4\sin^2\big(\frac{\alpha}{2}\big)\cos(\alpha)\big]\alpha'}{\sin^2(\alpha)}.$$

We use $4\sin\big(\frac{\alpha}{2}\big)\cos\big(\frac{\alpha}{2}\big) = 2\sin(\alpha)$ and $-4\sin^2\big(\frac{\alpha}{2}\big) = -2 + 2\cos(\alpha)$. With the Euler-Lagrange equation (30) this leads to

$$\begin{aligned} &-\frac{2\mu_c\cos(\alpha)\alpha'}{(\mu - \mu_c)\sin^2(\alpha)} + \frac{2\big[\sin^2(\alpha) - \cos(\alpha) + \cos^2(\alpha)\big]\alpha'}{\sin^2(\alpha)} \\ &\qquad = \frac{\big[2(\mu_c - \mu)\big(\sin(\alpha)\cos(\alpha)u' + \cos^2(\alpha) - \sin^2(\alpha)\big) + 2\mu\cos(\alpha)\big]\alpha'}{2\mu + (\mu_c - \mu)\cos^2(\alpha)} \end{aligned}$$

and simplifies to

$$\frac{\mu_c\cos(\alpha)\alpha'}{(\mu_c-\mu)(1-\cos^2(\alpha))}+\frac{\big[1-\cos(\alpha)\big]\alpha'}{1-\cos^2(\alpha)}$$
$$=\ \frac{\big[(\mu_c-\mu)\big(\sin(\alpha)\cos(\alpha)u'+\cos^2(\alpha)-\sin^2(\alpha)\big)+\mu\cos(\alpha)\big]\alpha'}{2\mu+(\mu_c-\mu)\cos^2(\alpha)}.$$

On the right we plug in the expression (49) for u'. So we obtain

$$\frac{\big[(\mu_c-\mu)\big(1-\cos(\alpha)\big)+\mu_c\cos(\alpha)\big]\alpha'}{(\mu_c-\mu)\big(1-\cos^2(\alpha)\big)}$$
$$=\ \frac{\big[-2\mu_c\cos(\alpha)+\mu\cos(\alpha)+(\mu_c-\mu)\big(2\cos(\alpha)-2\cos^2(\alpha)+\cos^2(\alpha)-\sin^2(\alpha)\big)\big]\alpha'}{2\mu+(\mu_c-\mu)\cos^2(\alpha)}.$$

After simplifications, this is equivalent to

$$\frac{\big[(\mu_c-\mu)+\mu\cos(\alpha)\big]\alpha'}{(\mu_c-\mu)\big(1-\cos^2(\alpha)\big)}=\frac{\big[-\mu\cos(\alpha)-(\mu_c-\mu)\big]\alpha'}{2\mu+(\mu_c-\mu)\cos^2(\alpha)}. \tag{50}$$

Expanding this, we find

$$\big[2\mu(\mu_c-\mu)+2\mu^2\cos(\alpha)+(\mu_c-\mu)^2\cos^2(\alpha)+\mu(\mu_c-\mu)\cos^3(\alpha)\big]\alpha'$$
$$=\ \big[-\mu(\mu_c-\mu)\cos(\alpha)-(\mu_c-\mu)^2+\mu(\mu_c-\mu)\cos^3(\alpha)+(\mu_c-\mu)^2\cos^2(\alpha)\big]\alpha'. \tag{51}$$

This simplifies further to

$$\big[2\mu^2+\mu(\mu_c-\mu)\big]\cos(\alpha)\alpha'=\big[2\mu(\mu-\mu_c)-(\mu_c-\mu)^2\big]\alpha' \tag{52}$$

and eventually

$$\mu(\mu+\mu_c)\cos(\alpha)\alpha'=(\mu+\mu_c)(\mu-\mu_c)\alpha'.$$

Hence either $\alpha'=0$ or

$$\alpha\equiv\alpha_4:=\arccos\Big(\frac{\mu-\mu_c}{\mu}\Big) \tag{53}$$

provided $\big|\frac{\mu-\mu_c}{\mu}\big|\le 1$. In both cases we have $\alpha'=0$ which shows with (30) that $u''=0$. □

Remark 2. *The consistent coupling condition is made such that the homogeneous deformation $\overline{u}(x)=\gamma x$ remains a solution of the boundary value problem.*

For given $\gamma > 0$ we introduce the constants

$$\alpha_1^- := \arctan\Big(\frac{\gamma\mu - f}{2\mu + \frac{\gamma}{2}f}\Big), \quad \alpha_1^+ := \arctan\Big(\frac{\gamma\mu + f}{2\mu - \frac{\gamma}{2}f}\Big), \quad \alpha_2 := \arctan\Big(\frac{\gamma}{2}\Big), \quad \alpha_3 := \eta^{-1}(\gamma) \tag{54}$$

where

$$f := \sqrt{(\gamma^2+4)(\mu-\mu_c)^2 - 4\mu^2}. \tag{55}$$

The *critical value of* μ_c is set as

$$\mu_c^{\rm crit} := \mu\Big[1 - \frac{2}{\sqrt{\gamma^2+4}}\Big]. \tag{56}$$

For later use we observe the relationship

$$\alpha_1^{\pm} = \arctan\Big(\frac{\gamma}{2}\Big) \pm \arctan\Big(\frac{f}{2\mu}\Big) = \alpha_2 \pm \arctan\Big(\frac{f}{2\mu}\Big). \tag{57}$$

Remark 3. *(i) Let $4\mu \neq \gamma f$ and $\mu_c \leq \mu_c^{\rm crit}$ for $\mu > \mu_c$ or $\mu_c \geq \mu\big(1 + \frac{2}{\sqrt{\gamma^2+4}}\big)$. Then α_1^-, α_1^+ are well-defined and solve*

$$\gamma\sin(\alpha) + 2\cos(\alpha) = \frac{2\mu}{\mu - \mu_c}. \tag{58}$$

(ii) For $\gamma < 2$, the constant α_3 has the alternative representation

$$\alpha_3 = \arctan\Big(\frac{4\gamma}{4-\gamma^2}\Big). \tag{59}$$

Proof. *(i) With $S := \sin(\alpha)$, $C := \cos(\alpha)$, $g := \frac{2\mu}{\mu-\mu_c}$, we find $2C = g - \gamma S$ implying $4C^2 = 4 - 4S^2 = (g - \gamma S)^2$. This leads to the quadratic equation*

$$S^2 - \frac{2\gamma g}{\gamma^2+4}S + \frac{g^2-4}{\gamma^2+4} = 0$$

with the solutions

$$S_\pm \;=\; \frac{\gamma g \pm \sqrt{\gamma^2 g^2 + (4-g^2)(\gamma^2+4)}}{\gamma^2+4} = \frac{\gamma g \pm 2d}{\gamma^2+4} \tag{60}$$

where $d := (\gamma^2 + 4 - g^2)^{1/2}$. Eqn. (60) and $2C = g - \gamma S$ imply

$$C_\pm = \frac{2g \mp \gamma d}{\gamma^2+4}$$

and (58) has the solutions

$$\alpha_1^- = \arctan\Big(\frac{S_-}{C_-}\Big), \qquad \alpha_1^+ = \arctan\Big(\frac{S_+}{C_+}\Big). \tag{61}$$

Writing

$$d = \frac{\left((\gamma^2+4)(\mu-\mu_c)^2 - 4\mu^2\right)^{1/2}}{(\mu-\mu_c)} =: \frac{f}{\mu-\mu_c}$$

we arrive at the defining identities (54) of $\alpha_1^{\pm}$*. The existence of* $\alpha_1^{\pm}$ *in (61) requires for* $\mu > \mu_c$

$$\gamma^2 + 4 \geq g^2 = \frac{4\mu^2}{(\mu-\mu_c)^2} \iff \mu_c^{\rm crit} := \mu\Big(1 - \frac{2}{\sqrt{\gamma^2+4}}\Big) \geq \mu_c. \tag{62}$$

(ii) In view of (21), the equation $\eta(\alpha_3) = \gamma$ *is equivalent to*

$$\gamma \sin(\alpha_3) + 2\cos(\alpha_3) = 2. \tag{63}$$

The calculus in (i) with $g := 2$ *entails* $d = \gamma$ *and* $\alpha = 0$, $\alpha = \arctan\left(\frac{2\gamma \pm 2\gamma}{4-\gamma^2}\right) = \alpha_3$ *as solutions of Eqn. (63).*

As minimizer of the Cosserat problem, $\alpha \equiv 0$ is only present if $\mu_c = 0$, but then $0 = \alpha_1^-$ which is why the zero solution is not part of (54).

Corollary 1. *Any solution* $u \in X := \{W^{2,2}(\Omega) \mid u(0) = 0,\, u(1) = \gamma\}$ *to (26) is monotonically increasing. The homogeneous function* $\overline{u}(x) := \gamma\, x$ *solves the Euler-Lagrange equations (30), (31). Depending on the values of* μ *and* μ_c*, the corresponding solution* α *to (30), (31) is given by*

$$\begin{aligned}
&\textit{(i) } \mu = \mu_c: && \alpha(x) \equiv \alpha_2. && (64)\\
& && (\overline{u}, \alpha_2) \textit{ is a local minimizer of } E.\\
&\textit{(ii) } \mu_c = 0: && \alpha(x) \equiv \alpha_1^- = 0,\ \alpha(x) \equiv \alpha_2,\ \alpha(x) \equiv \alpha_3. && (65)\\
& && (\overline{u}, 0) \textit{ and } (\overline{u}, \alpha_3) \textit{ are local minimizers of } E.\\
&\textit{(iii) } \mu_c > 0,\ \mu \neq \mu_c: && \alpha(x) \equiv \alpha_2,\ \alpha(x) \equiv \alpha_1^{\pm} \textit{ whenever } \alpha_1^{\pm} \textit{ exist.} && (66)\\
& && \textit{For } \mu_c > \mu_c^{\rm crit}, (\overline{u}, \alpha_2) \textit{ is a local minimizer of } E.\\
& && (\overline{u}, \alpha_1^{\pm}) \textit{ are local minimizers of } E \textit{ if } \mu > \mu_c,\ \mu_c \leq \mu_c^{\rm crit} \textit{ and } \alpha_1^{\pm} \neq \alpha_2.
\end{aligned}$$

Proof. Due to Lemma 3, any minimizer $u \in W^{2,2}(\Omega)$ to (26) must be piecewise linear. Choosing a function u with $u(0) = 0$, $u(1) = \gamma$ which is not monotonically increasing enlarges the component $\frac{\mu}{2}|u'|^2$ in W, cf. Eqn. (19). With (43), this demonstrates the optimality of $\overline{u}(x)$ in the class X of regular solutions. It remains to find the optimal values of α, and the strict positivity of the second variation $D^2_\alpha(\overline{u}, \alpha)$ is sufficient for that, see (75) below.

For fixed $u \in X$ and a test function $\delta\alpha \in C^\infty((0,1);\, \mathbb{R})$, the second variation of E with respect to α is

$$D^2_\alpha E(u,\alpha)(\delta\alpha, \delta\alpha) = \int_0^1 \Big(W_{\alpha\alpha}(u', \alpha, \alpha') - \frac{\rm d}{{\rm dx}} W_{\alpha\alpha'}(u', \alpha, \alpha')\Big)\delta\alpha(x)^2 + W_{\alpha'\alpha'}(u', \alpha, \alpha')\delta\alpha'(x)^2\, {\rm dx} \tag{67}$$

where subscripts denote partial derivatives. Here we have, cf. Eqn. (19),

$$W(u',\alpha,\alpha') = \frac{\mu}{2}|u'|^2 + \frac{\mu}{2}\Big(\sin(\alpha)u' - 4\sin^2\big(\frac{\alpha}{2}\big)\Big)^2 + \frac{\mu_c}{2}\Big(\cos(\alpha)u' - 2\sin(\alpha)\Big)^2$$

such that $W_{\alpha\alpha'}(u',\alpha,\alpha') = W_{\alpha'\alpha'}(u',\alpha,\alpha') = 0$. So the second variation (67) w.r.t. α simplifies to

$$D^2_\alpha E(u,\alpha)(\delta\alpha,\delta\alpha) = \int_0^1 W_{\alpha\alpha}(u',\alpha)\,\delta\alpha(x)^2\,\mathrm{dx}. \tag{68}$$

Here and below we simply write $W(u',\alpha)$ instead of $W(u',\alpha,\alpha')$ due to $L_c = 0$.

Direct computations reveal

$$\begin{aligned} W_\alpha(u',\alpha) &= \mu\Big(\sin(\alpha)u' - 4\sin^2\big(\tfrac{\alpha}{2}\big)\Big)\Big(\cos(\alpha)u' - 2\sin(\alpha)\Big) \\ &\quad - \mu_c\Big(\cos(\alpha)u' - 2\sin(\alpha)\Big)\Big(\sin(\alpha)u' + 2\cos(\alpha)\Big), \\ W_{\alpha\alpha}(u',\alpha) &= (\mu-\mu_c)\Big(\cos(\alpha)u' - 2\sin(\alpha)\Big)^2 + \mu_c\Big(\sin(\alpha)u' + 2\cos(\alpha)\Big)^2 \\ &\quad - \mu\Big(\sin(\alpha)u' - 4\sin^2\big(\tfrac{\alpha}{2}\big)\Big)\Big(\sin(\alpha)u' + 2\cos(\alpha)\Big). \end{aligned} \tag{69}$$

(i) For $\mu = \mu_c$, by direct investigation of (44), (45) we can verify that $(\overline{u},\alpha_2)$ solves the Euler-Lagrange equations. With (69) we find

$$\begin{aligned} W_{\alpha\alpha}(\overline{u}',\alpha_2) &= \mu\Big(\sin(\alpha_2)\gamma + 2\cos(\alpha_2)\Big)^2 - \mu\Big(\sin(\alpha_2)\gamma - 4\sin^2\big(\tfrac{\alpha_2}{2}\big)\Big)\Big(\sin(\alpha_2)\gamma + 2\cos(\alpha_2)\Big) \\ &= \mu\Big(\sin(\alpha_2)\gamma + 2\cos(\alpha_2)\Big)\Big(\sin(\alpha_2)\gamma + 2\cos(\alpha_2) - \sin(\alpha_2)\gamma + \underbrace{4\sin^2\big(\tfrac{\alpha_2}{2}\big)}_{=\,2-2\cos(\alpha_2)}\Big) \\ &= 2\mu\Big(\sin(\alpha_2)\gamma + 2\cos(\alpha_2)\Big) \\ &= (\gamma^2+4)\mu\cos(\alpha_2). \end{aligned} \tag{70}$$

Next we observe the identities

$$\cos(\arctan(t)) = \frac{1}{\sqrt{t^2+1}}, \qquad t \in \mathbb{R}, \tag{71}$$

$$\sin(\arctan(t)) = \frac{t}{\sqrt{t^2+1}}, \qquad t \in \mathbb{R}. \tag{72}$$

Consequently

$$\cos(\alpha_2) = \cos\Big(\arctan\Big(\frac{\gamma}{2}\Big)\Big) = \frac{2}{(\gamma^2+4)^{1/2}}, \tag{73}$$

$$\sin(\alpha_2) = \sin\Big(\arctan\Big(\frac{\gamma}{2}\Big)\Big) = \frac{\gamma}{(\gamma^2+4)^{1/2}} \tag{74}$$

such that

$$W_{\alpha\alpha}(\overline{u}', \alpha_2) = (\gamma^2+4)\mu\cos(\alpha_2) = 2\mu\sqrt{\gamma^2+4}.$$

With (68), this implies the strict positivity of the second variation w.r.t. α, i.e. there is a constant $K > 0$ such that

$$D^2_\alpha E(\overline{u}, \alpha_2)(\delta\alpha, \delta\alpha) \geq K\|\delta\alpha\|^2 \tag{75}$$

for any test function $\delta\alpha$, proving that $(\overline{u}, \alpha_2)$ is indeed a local minimizer of E, see, e.g. [20].

(ii) For $\mu_c = 0$, the Euler-Lagrange equations read

$$\Big[1 - \frac{\cos^2(\alpha)}{2}\Big]u'' = \big[\cos(\alpha) - \sin(\alpha)\cos(\alpha)u' + \sin^2(\alpha) - \cos^2(\alpha)\big]\alpha', \tag{76}$$

$$0 = \big(\cos(\alpha)u' - 2\sin(\alpha)\big)\Big(\sin(\alpha)u' - 4\sin^2\big(\frac{\alpha}{2}\big)\Big). \tag{77}$$

The definition (55) implies $f = \gamma\mu$ for $\mu_c = 0$, leading to $\alpha_1^- = 0$. Direct investigation of (76), (77) shows that $(\overline{u}, 0)$, $(\overline{u}, \alpha_2)$ and $(\overline{u}, \alpha_3)$ are solutions of the Euler-Lagrange equations. With (69) we find

$$\begin{aligned} W_{\alpha\alpha}(\overline{u}', 0) &= \mu\gamma^2 > 0, \\ W_{\alpha\alpha}(\overline{u}', \alpha_3) &= \mu\Big(\cos(\alpha_3)\gamma - 2\sin(\alpha_3)\Big)^2. \end{aligned}$$

Hence $W_{\alpha\alpha}(\overline{u}', \alpha_3) = 0$ only if $\cos(\alpha_3)\gamma = 2\sin(\alpha_3)$ or equivalently $\alpha_3 := \eta^{-1}(\gamma) = \arctan\big(\frac{\gamma}{2}\big)$, i.e. only if $\gamma = \eta\big(\arctan(\gamma/2)\big)$, i.e. only if

$$\gamma = \frac{4\sin^2\big(\frac{\arctan(\gamma/2)}{2}\big)}{\sin(\arctan(\gamma/2))} = \frac{2 - 2\cos(\arctan(\gamma/2))}{\sin(\arctan(\gamma/2))} \tag{78}$$

where (21) was used. With (71) and (72), Eqn. (78) becomes

$$\gamma = \frac{2 - \frac{2}{\sqrt{1+\gamma^2/4}}}{\frac{\gamma/2}{\sqrt{1+\gamma^2/4}}} = \frac{2\sqrt{1+\frac{\gamma^2}{4}} - 2}{\gamma/2} \iff \gamma^2 = 4\sqrt{1+\frac{\gamma^2}{4}} - 4 \iff \gamma^2 + 4 = 2\sqrt{4+\gamma^2}.$$

The last equality is only satisfied for $\gamma = 0$, proving $W_{\alpha\alpha}(\overline{u}', \alpha_3) > 0$ for $\gamma \neq 0$ which yields as in (i) the strict positivity (75) of the second variation w.r.t. α such that $(\overline{u}, \alpha_1^-)$ and $(\overline{u}, \alpha_3)$ are local minimizers of E.

(iii) For $\mu > 0$, $\mu_c > 0$, $\mu \neq \mu_c$, Lemma 3, Case 1 in (ii) shows that $(\overline{u}, \alpha_2)$ solves the Euler-Lagrange equations (30), (31). As for the second factor in Eqn. (31),

$$(\mu - \mu_c)\big(\sin(\alpha)\gamma + 2\cos(\alpha) - 2\big) - 2\mu_c = 0 \iff \sin(\alpha)\gamma + 2\cos(\alpha) = \frac{2\mu}{\mu - \mu_c}.$$

Hence, by virtue of Remark 3, $(\overline{u}, \alpha_1^-)$ and $(\overline{u}, \alpha_1^+)$ solve the Euler-Lagrange equations (30), (31) whenever $\alpha_1^\pm$ exist.

In order to investigate when $(\overline{u},\alpha_2)$ is a local minimizer of E, we once more inspect the second variation (68) of E w.r.t. α. Starting from (69) we find

$$\begin{aligned} W_{\alpha\alpha}(\overline{u}',\alpha_2) &= (\mu-\mu_c)\big(\underbrace{\cos(\alpha_2)\gamma-2\sin(\alpha_2)}_{=0}\big)^2+\mu_c\big(\sin(\alpha_2)\gamma+2\cos(\alpha_2)\big)^2 \\ &\quad -\mu\Big(\sin(\alpha_2)\gamma\underbrace{-4\sin^2\big(\frac{\alpha_2}{2}\big)}_{=2\cos(\alpha_2)-2}\Big)\big(\sin(\alpha_2)\gamma+2\cos(\alpha_2)\big) \\ &= (\mu_c-\mu)\big(\sin(\alpha_2)\gamma+2\cos(\alpha_2)\big)^2+2\mu\big(\underbrace{\sin(\alpha_2)\gamma+2\cos(\alpha_2)}_{=\frac{\gamma^2+4}{2}\cos(\alpha_2)}\big) \\ &= \frac{\gamma^2+4}{2}\cos(\alpha_2)\Big[2\mu+(\mu_c-\mu)\big(\sin(\alpha_2)\gamma+2\cos(\alpha_2)\big)\Big]. \end{aligned} \tag{79}$$

Using the formulas (73), (74) in (79), this yields

$$\begin{aligned} W_{\alpha\alpha}(\overline{u}',\alpha_2) &= \frac{\gamma^2+4}{2}\frac{2}{\sqrt{\gamma^2+4}}\Big[2\mu+(\mu_c-\mu)\Big(\frac{\gamma^2}{\sqrt{\gamma^2+4}}+\frac{4}{\sqrt{\gamma^2+4}}\Big)\Big] \\ &= \sqrt{\gamma^2+4}\Big[2\mu+(\mu_c-\mu)\sqrt{\gamma^2+4}\Big]. \end{aligned}$$

This shows the strict positivity (75) of $D^2_\alpha E(\overline{u},\alpha_2)(\delta\alpha,\delta\alpha)$ provided $\mu_c>\mu_c^{\rm crit}$.

From Eqns. (71), (72),

$$\gamma\sin(\alpha_1^-)+2\cos(\alpha_1^-)=\frac{2\mu}{\mu-\mu_c},\quad \gamma\cos(\alpha_1^-)-2\sin(\alpha_1^-)=\frac{f}{\mu-\mu_c}, \tag{80}$$

$$\gamma\sin(\alpha_1^+)+2\cos(\alpha_1^+)=\frac{2\mu}{\mu-\mu_c},\quad \gamma\cos(\alpha_1^+)-2\sin(\alpha_1^+)=\frac{-f}{\mu-\mu_c}. \tag{81}$$

Owing to the identity (69), this yields

$$\begin{aligned} W_{\alpha\alpha}(\gamma,\alpha_1^-)=W_{\alpha\alpha}(\gamma,\alpha_1^+) &= (\mu-\mu_c)\frac{f^2}{(\mu-\mu_c)^2}+\mu_c\frac{4\mu^2}{(\mu-\mu_c)^2}-\mu\Big(\frac{2\mu}{\mu-\mu_c}-2\Big)\frac{2\mu}{\mu-\mu_c} \\ &= \frac{f^2}{\mu-\mu_c}+\frac{4\mu^2\mu_c}{(\mu-\mu_c)^2}-\frac{2\mu^2}{\mu-\mu_c}\frac{2\mu_c}{\mu-\mu_c}=\frac{f^2}{\mu-\mu_c}. \end{aligned} \tag{82}$$

For $\mu>\mu_c$ and $f\neq 0$, this proves that $(\overline{u},\alpha_1^\pm)$ are local minimizers of E while for $f=0$, it holds $\alpha_1^\pm=\arctan(\frac{\gamma}{2})=\alpha_2$ due to (57). For $\mu_c<\mu_c^{\rm crit}$, Eqn. (62) holds with strict inequality such that

$$\begin{aligned} W_{\alpha\alpha}(\gamma,\alpha_2) &= 2\mu(\gamma^2+4)^{1/2}+(\mu-\mu_c)\big[0-(\gamma^2+4)\big] \\ &= (\gamma^2+4)^{1/2}\big[2\mu-(\mu-\mu_c)(\gamma^2+4)^{1/2}\big] \\ &< (\gamma^2+4)^{1/2}\big[2\mu-2\mu\big]=0 \end{aligned} \tag{83}$$

and $(\overline{u},\alpha_2)$ is no minimizer of E for $\mu_c<\mu_c^{\rm crit}$. □

Remark 4. *We point out that the solution $(\overline{u},\alpha_4)$ of the Euler-Lagrange equations found in Lemma 3, (ii) is not an independent case. The solution $(\overline{u},\alpha_4)$ requires $\left|\frac{\mu-\mu_c}{\mu}\right| \leq 1$, cf. Eqn. (53), and then, by the very definition of Case 2 in Lemma 3,*

$$\begin{aligned}\sin(\alpha_4)\gamma &= 4\sin^2\big(\frac{\alpha_4}{2}\big)+\frac{2\mu_c}{\mu-\mu_c} = 2-2\cos(\alpha_4)+\frac{2\mu_c}{\mu-\mu_c}\\ &= 2-\frac{2(\mu-\mu_c)}{\mu}+\frac{2\mu_c}{\mu-\mu_c} = \frac{2\mu_c}{\mu}+\frac{2\mu_c}{\mu-\mu_c} = \frac{2\mu_c(2\mu-\mu_c)}{\mu(\mu-\mu_c)}. \end{aligned} \tag{84}$$

Due to the relationship

$$\sin(\arccos(t)) = \sqrt{1-t^2} \qquad \text{for } t\in[-1,+1], \tag{85}$$

this yields

$$\sin(\alpha_4) = \sqrt{1-\frac{(\mu-\mu_c)^2}{\mu^2}} = \frac{1}{\mu}\sqrt{\mu_c(2\mu-\mu_c)}. \tag{86}$$

With (84) we obtain

$$\gamma = \frac{2\mu_c(2\mu-\mu_c)}{\mu(\mu-\mu_c)\sin(\alpha_4)} = \frac{2\mu_c(2\mu-\mu_c)}{\mu(\mu-\mu_c)}\,\frac{\mu}{\sqrt{\mu_c(2\mu-\mu_c)}} = \frac{2\sqrt{\mu_c(2\mu-\mu_c)}}{\mu-\mu_c}. \tag{87}$$

For γ given by (87), we have

$$\begin{aligned}\gamma\cos(\alpha_4)-2\sin(\alpha_4) &= \gamma\,\frac{\mu-\mu_c}{\mu}-\frac{2}{\mu}\sqrt{\mu_c(2\mu-\mu_c)}\\ &= \frac{2\sqrt{\mu_c(2\mu-\mu_c)}}{\mu-\mu_c}\,\frac{\mu-\mu_c}{\mu}-\frac{2}{\mu}\sqrt{\mu_c(2\mu-\mu_c)} = 0,\end{aligned}$$

leading to $\gamma\cos(\alpha_4)=2\sin(\alpha_4)$ or equivalently $\frac{\gamma}{2}=\tan(\alpha_4)$. This shows

$$\alpha_4 = \arctan\Big(\frac{\gamma}{2}\Big) = \alpha_2 \tag{88}$$

for γ given by (87).

In order to have $\gamma>0$ in (87), it must hold $0<\mu_c<\mu$, and the condition $\left|\frac{\mu-\mu_c}{\mu}\right|\leq 1$ is automatically satisfied.

Remark 5. *The following table lists the mechanical energies corresponding to the local minimizers of Corollary 1.*

$$\text{(i) } \mu=\mu_c: \quad E(\overline{u},\alpha_2) = \mu\Big[\gamma^2+4-2\sqrt{\gamma^2+4}\Big]. \tag{89}$$

$$\text{(ii) } \mu_c=0: \quad E(\overline{u},\alpha_1^-) = E(\overline{u},\alpha_3) = \frac{\mu}{2}\gamma^2. \tag{90}$$

$$\text{(iii) } \mu_c>0,\ \mu\neq\mu_c: \quad E(\overline{u},\alpha_2) = \mu\Big[\gamma^2+4-2\sqrt{\gamma^2+4}\Big] \text{ if } \mu_c>\mu_c^{\rm crit}. \tag{91}$$

$$E(\overline{u},\alpha_1^\pm) = \frac{\mu+\mu_c}{2}\gamma^2-\frac{2\mu_c^2}{\mu-\mu_c} \text{ whenever } \alpha_1^\pm \text{ exist and } \alpha_1^\pm\neq\alpha_2. \tag{92}$$

Remark 6. *We want to investigate whether* $(\overline{u},\alpha_2)$ *is a minimizer of* E *in the situation of Remark 4, i.e. if*

$$0<\mu_c<\mu \text{ and } (\mu-\mu_c)\gamma=2\sqrt{\mu_c(2\mu-\mu_c)}. \tag{93}$$

As $\overline{u}'(x)\equiv\gamma$ *and assuming that* $\alpha(x)\equiv a$ *for constant* $a\in\mathbb{R}$ *and* $x\in(0,1)$*, it is enough to investigate the real function*

$$f(a):=W(\overline{u},a)=\frac{\mu}{2}\gamma^2+\frac{\mu}{2}\Big(\gamma\sin(a)-4\sin^2\big(\frac{a}{2}\big)\Big)^2+\frac{\mu_c}{2}\Big(\gamma\cos(a)-2\sin(a)\Big)^2,$$

cf. the definition of W *in (19). Straightforward computations yield*

$$\begin{aligned}
f'(a) &= \big(\gamma\cos(a)-2\sin(a)\big)\big[(\mu-\mu_c)\big(\gamma\sin(a)+2\cos(a)\big)-2\mu\big],\\
f''(a) &= (\mu-\mu_c)\big[\big(\gamma\cos(a)-2\sin(a)\big)^2-\big(\gamma\sin(a)+2\cos(a)\big)^2\big]+2\mu\big(\gamma\sin(a)+2\cos(a)\big),\\
f'''(a) &= \big(\gamma\cos(a)-2\sin(a)\big)\big[2\mu-4(\mu-\mu_c)\big(\gamma\sin(a)+2\cos(a)\big)\big],\\
f^{(4)}(a) &= 4(\mu-\mu_c)\big[\big(\gamma\sin(a)+2\cos(a)\big)^2-\big(\gamma\cos(a)-2\sin(a)\big)^2\big]-2\mu\big(\gamma\sin(a)+2\cos(a)\big).
\end{aligned}$$

Remarkably, $f'(\alpha_2)=f''(\alpha_2)=f'''(\alpha_2)=0$*, but*

$$f^{(4)}(\alpha_2)=\frac{12\mu^2}{\mu-\mu_c}>0,$$

showing that α_2 *is a minimizer of* f *and indicating that* $(\overline{u},\alpha_2)$ *is a local minimizer of* E *for constant* $\alpha(x)\equiv\alpha_2$ *under the choice of parameters (93). The minimal energy coincides with (91) for* γ *given by (87). Due to* $f'(\alpha_2)=f''(\alpha_2)=f'''(\alpha_2)=0$*, the function* f *is extremely flat near* α_2*, making it very difficult to numerically compute the correct minimizer, see Fig. 6.*

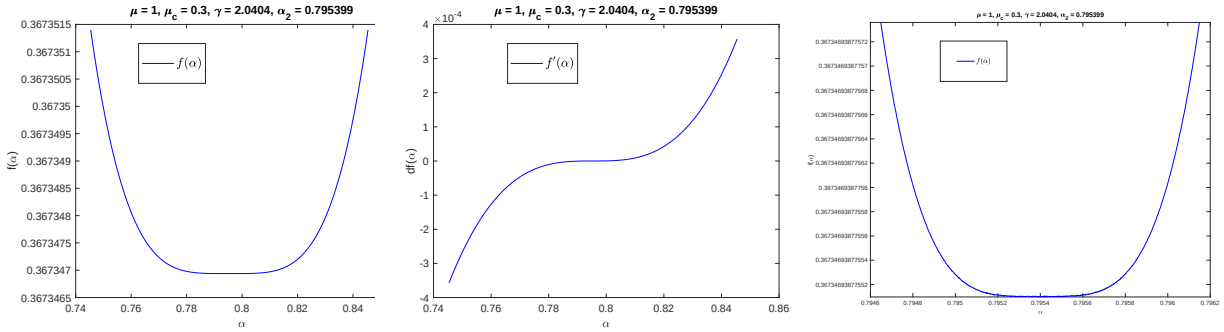


Figure 6: Left and center: Plot of $f(\alpha)$, $f'(\alpha)$ near α_2 for $\mu=1$, $\mu_c=0.3$ and γ given by (87). Right: Close-up of $f(\alpha)$ near α_2. The tiny oscillations of the graph near α_2 in the close-up are numerical rendering artifacts generated by MATLAB.

Remark 7. *Let $\mu > 0$ and $\gamma > 0$ be given. Corollary 1 states that the value of μ_c selects the minimizer of $E(\overline{u}, \cdot)$. For $\mu_c > \mu_c^{\mathrm{crit}}$, $(\overline{u}, \alpha_2)$ is optimal while for $\mu_c < \mu_c^{\mathrm{crit}}$ and $\mu > \mu_c$, $(\overline{u}, \alpha_1^{\pm})$ are local minimizers. These findings are confirmed by our numerical simulations, cf. Fig. 12.*

Remark 8. *It is instructive to compare Corollary 1 and Remark 5 with the results in [17], stating that*

$$\text{For } \mu_c \geq \mu > 0: \qquad W_{\mu,\mu_c}(R;F) \sim W_{1,1}(R;F), \tag{94}$$

$$\text{For } \mu > \mu_c \geq 0: \qquad W_{\mu,\mu_c}(R;F) \sim W_{1,0}(R;\widetilde{F}_{\mu,\mu_c}). \tag{95}$$

Here, $F = D\varphi \in \mathbb{R}^{n\times n}$ is a given deformation gradient, $\widetilde{F}_{\mu,\mu_c} := \frac{\mu-\mu_c}{\mu}F$,

$$f \sim g :\Longleftrightarrow \operatorname*{argmin}_{R\in\mathrm{SO}(n)} f(R) = \operatorname*{argmin}_{R\in\mathrm{SO}(n)} g(R)$$

for two functions f and g, and

$$W_{\mu,\mu_c}(R;F) := \mu\big|\operatorname{sym}(R^TF - \mathbb{1}_3)\big|^2 + \mu_c\big|\operatorname{skew}(R^TF - \mathbb{1}_3)\big|^2 \tag{96}$$

which coincides with (19) for $L_c = 0$, F given by (12), and $R \in \mathrm{SO}(3)$ defined by (13).

In the classical parameter range $\mu_c \geq \mu > 0$,

$$\begin{aligned} W_{1,1}(R;F) &= \frac{1}{2}\Big[\gamma^2 + (\gamma\sin(\alpha) + 2\cos(\alpha) - 2)^2 + (\gamma\cos(\alpha) - 2\sin(\alpha))^2\Big] \\ &\sim \Big(\gamma\sin(\alpha) + 2\cos(\alpha) - 2\Big)\Big)^2 + \Big(\gamma\cos(\alpha) - 2\sin(\alpha)\Big)^2. \end{aligned}$$

The value $\alpha_3 = \eta^{-1}(\gamma)$ corresponds to the zeros of the first quadratic term on the right, the global minimizer α_2 to the zeros of the second quadratic term. This includes the case $\mu = \mu_c$.

Similarly, for the non-classical parameter range $\mu > \mu_c \geq 0$, introducing the scaling parameter $r = r_{\mu,\mu_c} := \frac{\mu-\mu_c}{\mu}$, direct inspection reveals

$$\begin{aligned} W_{1,0}(R;\widetilde{F}) &= \frac{1}{2}\Big(\gamma r\sin(\alpha) + 2r\cos(\alpha) - 2\Big)^2 + \frac{1}{2}\gamma^2r^2 + (r-1)^2 \\ &\sim \Big(\gamma\sin(\alpha) + 2\cos(\alpha) - \frac{2}{r}\Big)^2 = \Big(\gamma\sin(\alpha) + 2\cos(\alpha) - \frac{2\mu}{\mu-\mu_c}\Big)^2 \text{ for } \mu \neq \mu_c. \end{aligned} \tag{97}$$

The zeros on the right are the global minimizers $\alpha_1^{\pm}$ whenever they exist. Especially, for $\mu_c = 0$, Eqn. (97) with the help of (21) states that

$$W_{1,0}(R;\widetilde{F}) \sim \Big(\gamma\sin(\alpha) - 4\sin^2\big(\frac{\alpha}{2}\big)\Big)^2.$$

As outlined in Remark 3, the right hand side is zero (and minimal) for $\alpha = 0 = \alpha_1^-$ and for $\alpha = \alpha_3$ corresponding to (65).

In conclusion, Corollary 1 and Remark 5 confirm the results in [17].

4. Numerical simulations for vanishing internal length scale

For $L_c > 0$, various advanced numerical tools such as multigrid methods are available, [8]. We will not discuss this here. In contrast, the case $L_c = 0$ is numerically challenging as the regularizing term $2\mu L_c^2|\alpha'|^2$ in E and E_{red} disappears in the limit. We investigate the problem in two different ways and compare the solution strategies. We begin with the situation of non-regular solutions with $\alpha \in L^4(\Omega)$.

① Newton-GMRES algorithm

For $L_c = \mu_c = 0$ and $\alpha \in L^4(\Omega)$, the solutions (u, α) to $E_{\mathrm{red}}(u, \alpha) \to \min$ satisfy pointwise for $x \in \Omega = (0, 1)$ the two purely algebraic equations (see [31, Eqn. (3.30)] for a derivation),

$$\alpha(\alpha - u')\Big(\alpha - \frac{u'}{2}\Big) = 0, \tag{98}$$

$$(u' - \zeta)\Big(u' + \frac{1}{8}(u')^3 - \zeta\Big) = 0 \tag{99}$$

subject to the boundary conditions

$$u(0) = 0, \quad u(1) = \gamma, \quad u'(0) = u'(1), \quad \alpha(0) = \alpha(1) = \alpha_D \tag{100}$$

for a constant $\alpha_D \in \mathbb{R}$ and with $\zeta := (1 + \alpha_D^2)u'(0) - \alpha_D^3$.

In general, there is a multitude of solutions to (98)–(100). In order to specify a solution, one may prescribe a volume fraction $\theta \in [0, 1]$ such that

$$\mathcal{L}^1\big(\{x \in \Omega \mid \alpha(x) = 0\}\big) = \theta, \tag{101}$$

where $\mathcal{L}^1$ denotes the one-dimensional Lebesgue measure.

In order to compute solutions to (98)–(100), the derivative u' is approximated by central difference quotients leading to a discrete problem in the standard form

$$\text{Find } x \in \mathbb{R}^{2N-3} : \quad G(x) = 0 \tag{102}$$

for a differentiable function $G : \mathbb{R}^{2N-3} \mapsto \mathbb{R}^{2N-3}$ and with $N \in \mathbb{N}$ denoting the number of discretization points in Ω. The solutions to (102) are computed using a Newton-GMRES method where the Fréchet derivative DG of G is approximated by

$$DG(x)d \sim \frac{G(x + \delta d) - G(x)}{\delta} \tag{103}$$

for suitable small $\delta > 0$ and GMRES is used to solve the linearized equations. While the algorithm computes DG automatically thanks to Eqn. (103), its practicability is limited by the huge memory requirements.
The implementation details related to the definition of G are left out here.

② BFGS Quasi-Newton method

As in the first method, the values of α, α' and u' are discretized along $N \in \mathbb{N}$ points $z_i \in \Omega$. Letting $f_i := W(u'(z_i), \alpha(z_i), \alpha'(z_i))$ be the integrand either in (18) or in (24), the repeated Trapezoidal rule

$$\left(\frac{1}{2}f_1 + \sum_{i=2}^{N-1} f_i + \frac{1}{2}f_N\right)$$

is used for the approximate integration. The minimization of the functional is carried out by a Quasi-Newton method where the approximate Hessian is computed by the Broyden-Fletcher-Goldfarb-Shanno update formula, [10]. Again, we leave out the implementation details, but refer to [5, 6, 7], where the limited-memory variant of the algorithm is applied to Cosserat plasticity and recrystallization.

In comparison, both algorithms compute the same solutions. However, the BFGS Quasi-Newton method is capable of handling larger values of N due to the tremendous memory needs of the Newton-GMRES scheme.

Fig. 7 displays three minimizers of E_{red} in $\mathcal{X}^D$ for different values of N and prescribed slope $u'(0)$ at the boundary. The deformation u_N forms a sawtooth pattern with alternating, constant slopes, while the values of α randomly concentrate at 0 and γ. The computations of Fig. 7 suggest further that u_N converges to the homogeneous deformation $\overline{u}(x) := \gamma\, x$ as $N \to \infty$.

Fig. 8 and Fig. 9 compare the minimizers of E_{red} in $\mathcal{X}^C$ and $\mathcal{X}^D$ for three different values of N. Again, α randomly concentrates at 0 and γ while the deformation u_N forms a sawtooth pattern with alternating, constant slopes. The computed deformation u is extremely close to $\overline{u}$ but energetically beats the homogeneous solution.

We will adopt the following notation in the set $\mathcal{M}^+(\mathbb{R})$ of finite positive *Radon measures*. For a sequence $(v_j)_{j\in\mathbb{N}}$ and a Carathéodory function f such that

$$f(x, v_j) \rightharpoonup \left(x \mapsto \int_{\mathbb{R}} f(x, A)\, \mathrm{d}\nu_x(A)\right) \quad \text{in } L^1(\mathbb{R})$$

for a parameterized measure $\nu = (\nu_x)_{x\in\mathbb{R}}$ we use the shorthand notation $v_j \overset{Y}{\to} \nu$.

Remark 9. *The numerical computations in Figs. 7–9 indicate the following result regarding non-regular solutions.*

Let $L_c = 0$ and $(u_N, \alpha_N)_{N\in\mathbb{N}}$ be a minimizing sequence of E_{red} in $W^{1,2}(\Omega) \times L^4(\Omega)$ with $u_N(x) \rightharpoonup \overline{u}(x)$, $\alpha_N \rightharpoonup \alpha$ for $N \to \infty$. Then, there is a (not relabelled) subsequence and a constant $\theta \in [0, 1]$ such that

$$W_{\mathrm{red}}(u_N, \alpha_N) \overset{Y}{\to} \theta\delta_0 + (1-\theta)\delta_\gamma. \tag{104}$$

The existence of a limiting Young measure generated by the subsequence (u_N, α_N) can be made rigorous by applying the fundamental theorem of Young measures, see e.g. [24]. We observe that the family $(W_{\mathrm{red}}(u_N, \alpha_N))_{N\in\mathbb{N}}$ is uniformly bounded in L^1 and equi-integrable by the Dunford-Pettis theorem.

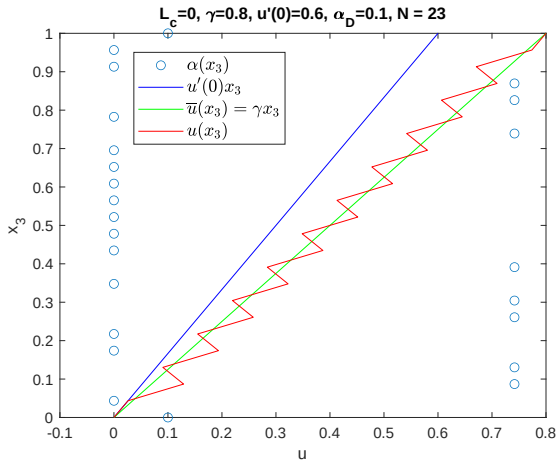
Fig. 10 displays minimizers of E in $\mathcal{X}^C$. Except near $\partial\Omega = \{0, 1\}$, the minimizing rotation α takes constant values with either $\alpha \equiv \alpha_1^- := 0$ or $\alpha \equiv \alpha_3 := \eta^{-1}(\gamma)$ in accordance with Corollary 1 (ii). Depending on the initial values at start of the optimization, the BFGS-algorithm computes one of two different minimizers u which both converge in Ω to $\overline{u}(x)$ as $N \to \infty$. The first, u_1 with $\alpha \equiv \alpha_1^-$, is a straight line except near $\partial\Omega$. The second, u_2 with $\alpha \equiv \alpha_3$, leads to a scaled function $u_{\mathrm{scale}}(x) := \gamma\, x + N\big(u_2(x) - \gamma\, x\big)$ which is a bended curve, see Fig. 10. The energy levels of both computed local minimizers are extremely close with

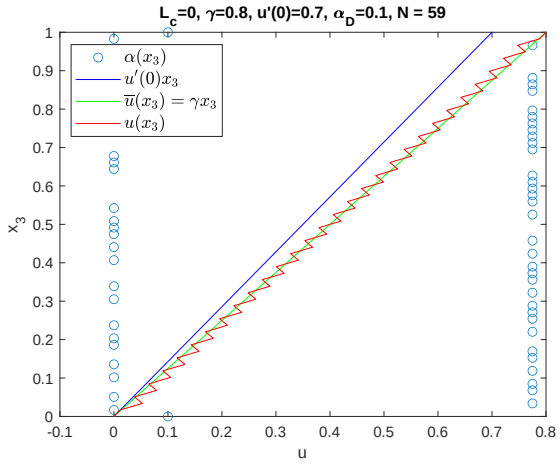
$$E(u_1, \alpha_1^-) = 0.32001744, \qquad E(u_2, \alpha_3) = 0.320018, \tag{105}$$

confirming Eqn. (90). Yet, numerical optimization favors $(\overline{u}, \alpha_1^-)$ over $(\overline{u}, \alpha_3)$, underlining that the energy landscape for geometrically nonlinear Cosserat materials is extremely complicated and emphasizing why it is so hard to numerically compute the correct global minimizers. In comparison to (105), the theoretical infimal energy is $E(\overline{u}, \alpha_1^-) = \frac{\mu}{2}\gamma^2 = 0.32$, but $(\overline{u}, \alpha_1^-)$ violates the consistent coupling condition (27).

Fig. 11 studies minimizers in $\mathcal{X}^C$ related to Corollary 1, (i). Again, $u_N \to \overline{u}$ in Ω for $N \to \infty$. The minimizing microrotation angle α is constant (except near $\partial\Omega$) and takes the values predicted by Cor. 1.

Fig. 12 confirms the validity of Corollary 1, (iii) and demonstrate that $(\overline{u}, \alpha_1^{\pm})$ and $(\overline{u}, \alpha_2)$ are the local minimizers of E depending on the value of μ_c.





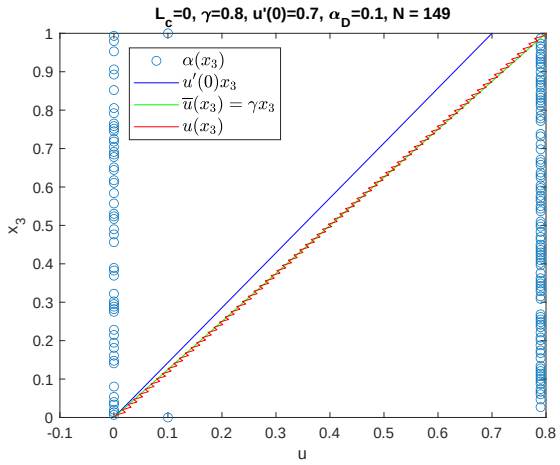


Figure 7: Minimizers of E_{red} in $\mathcal{X}^D$ for $N = 23$, $N = 59$ and $N = 149$ for $\mu = 1$, $\mu_c = 0$, $\gamma = 0.8$, prescribed $u'(0) = u'(1)$ (blue line) and $\alpha_D = u(0) = u(1) = 0.1$. The blue balls are the computed values of α randomly concentrating at 0 and γ. The green line displays the homogeneous deformation $\overline{u}(x) = \gamma\, x$. The deformation u is rendered in red forming a microstructure with a sawtooth pattern.

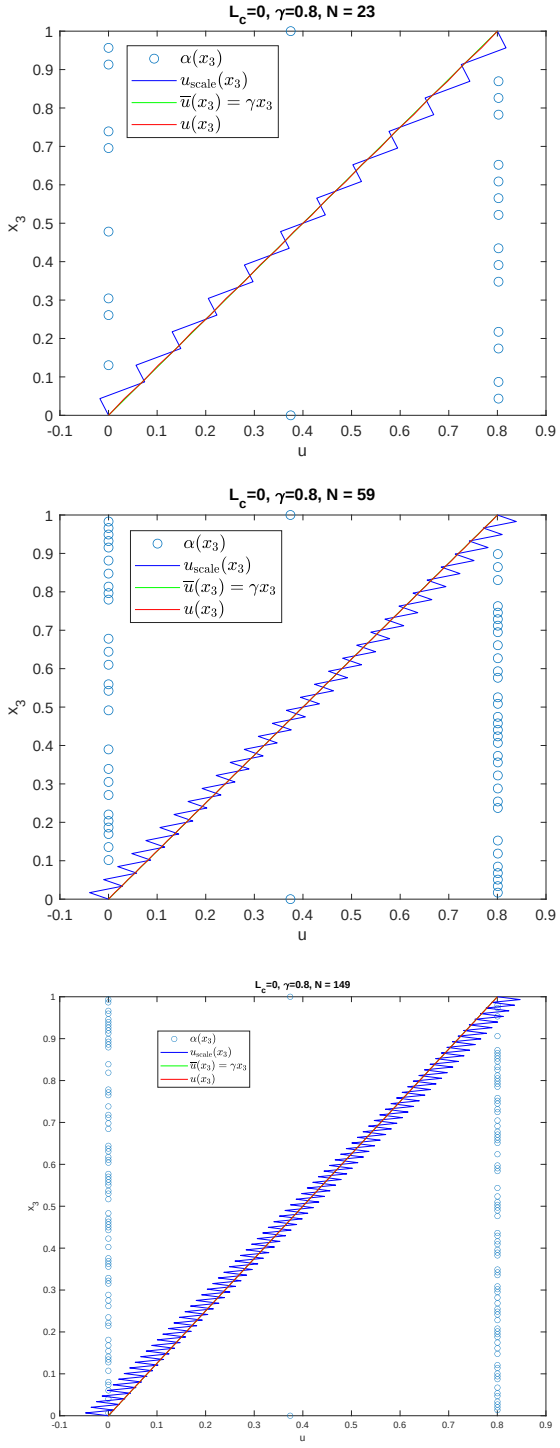
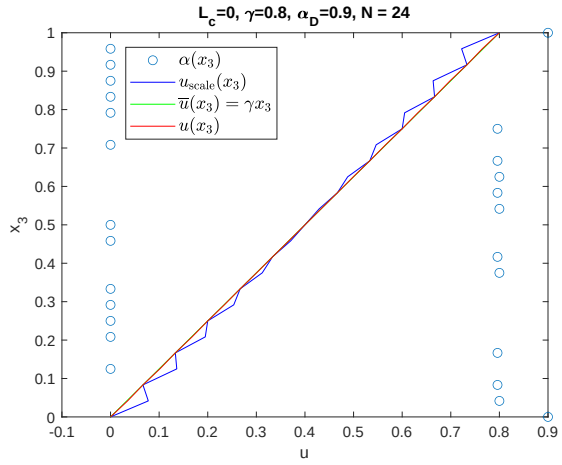
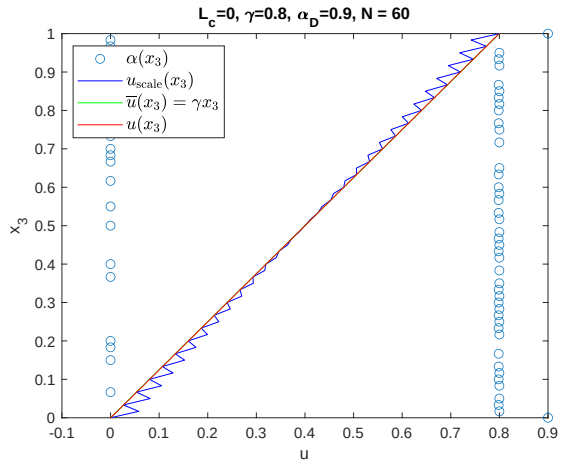


Figure 8: Minimizers of E_{red} in $\mathcal{X}^C_{\text{red}}$ for $N = 23$, $N = 59$ and $N = 149$ for $\mu = 1$, $\mu_c = 0$, $\gamma = 0.8$. The blue balls are the computed values of α randomly concentrating at 0 and γ. The deformation u is rendered in red and forms a microstructure with a sawtooth pattern which is extremely close to the homogeneous deformation $\overline{u}(x) = \gamma\, x$ rendered in green. The differences between u and $\overline{u}$ is amplified by the blue line rendering the rescaled deformation $u_{\text{scale}}(x) := \gamma\, x + N(u(x) - \gamma x)$. The value $\alpha(0)$ is strictly smaller than $\frac{\gamma}{2}$ and indicates by which amount the sawtooth solution u energetically beats the homogeneous solution.





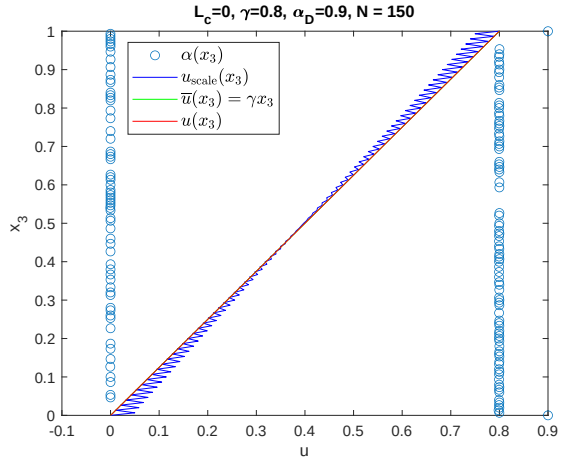


Figure 9: Minimizers of E_{red} in $\mathcal{X}^D$ for $N = 24$, $N = 60$ and $N = 150$ for $\mu = 1$, $\mu_c = 0$, $\gamma = 0.8$. The blue balls are the computed values of α randomly concentrating at 0 and γ. The deformation u is rendered in red and forms a microstructure with a sawtooth pattern which is extremely close to the homogeneous deformation $\overline{u}(x) = \gamma\, x$ rendered in green. The blue line is the rescaled deformation $u_{\text{scale}}(x) := \gamma\, x + N(u(x) - \gamma\, x)$ amplifying the differences between u and $\overline{u}$. As can be seen, the oscillation of u is largest near $\partial\Omega$ and smallest at $x = 0.5$.

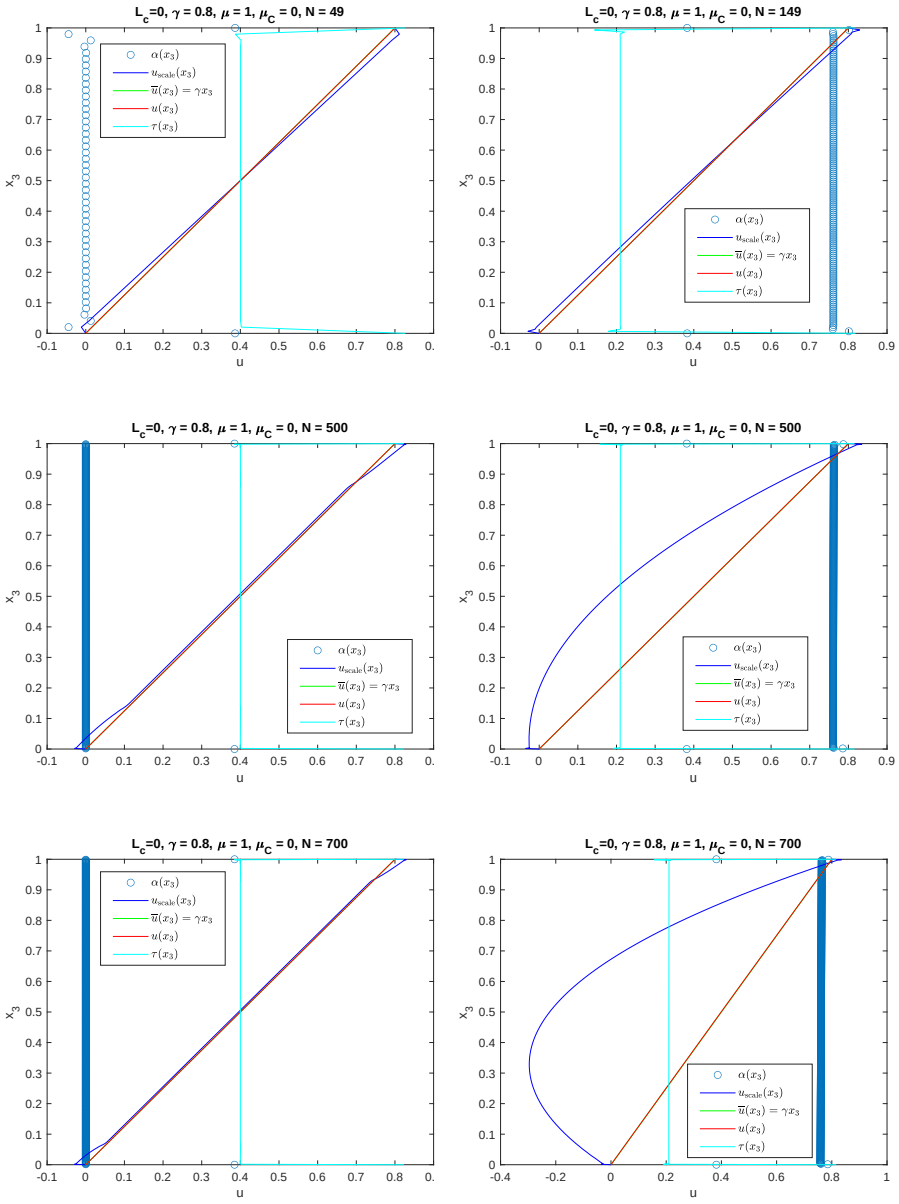


Figure 10: Minimizers of E in $\mathcal{X}^C$ for $\mu = 1$, $\mu_c = 0$, $\gamma = 0.8$ and $N = 49$, $N = 149$, $N = 500$, $N = 700$. The blue balls are the computed values of α with either $\alpha \equiv \alpha_1^- = 0$ or $\alpha \equiv \alpha_3 = \eta^{-1}(\gamma) = 0.760053$. In cyan the computed stress tensor τ which is constant in Ω. The deformation u is rendered in red, extremely close to $\overline{u}(x) = \gamma\, x$ rendered in green. The blue line is the rescaled deformation $u_{\rm scale} := \gamma\, x + N(u(x) - \gamma\, x)$.

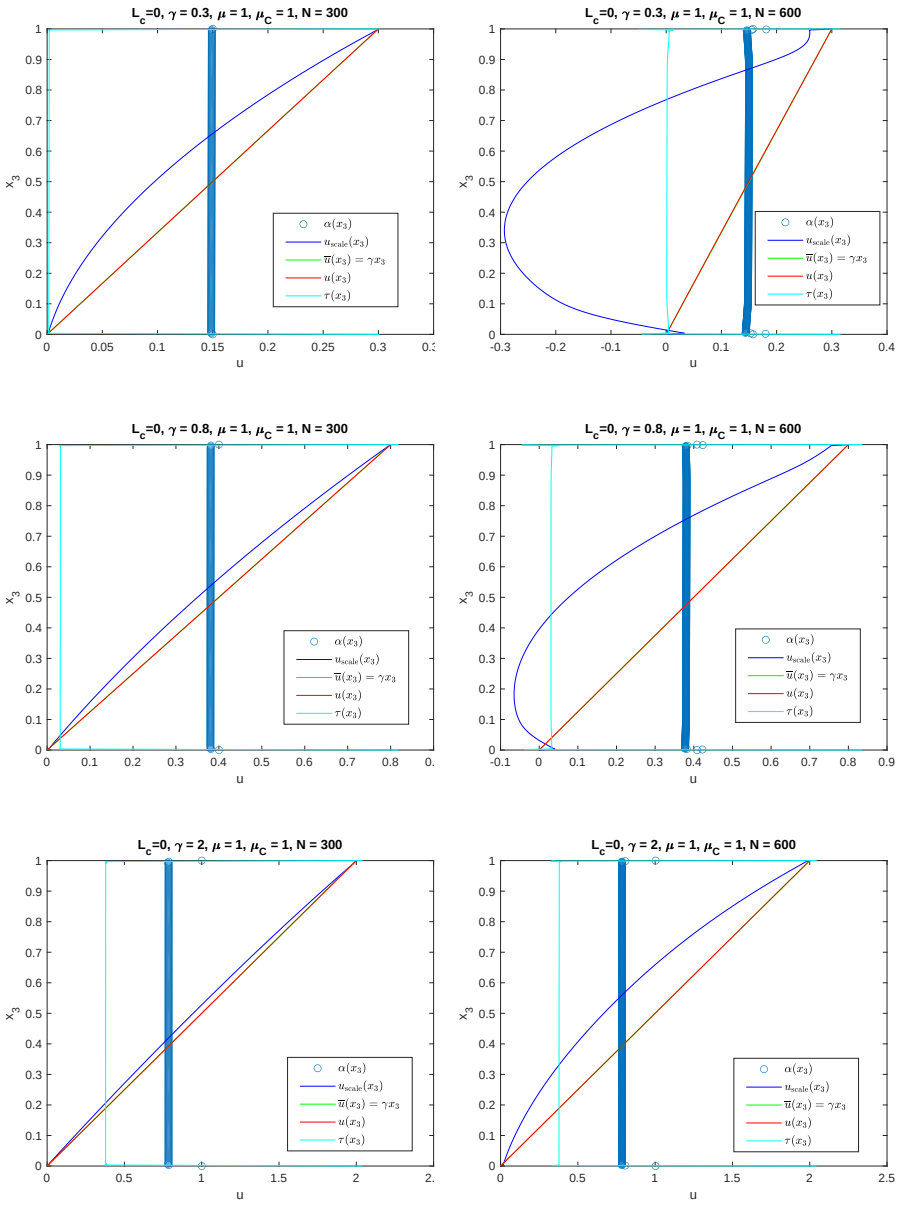


Figure 11: Minimizers of E in $\mathcal{X}^C$ for $\mu = \mu_c = 1$ and $N = 300$ (left), $N = 600$ (right) and $\gamma = 0.3$ top line, $\gamma = 0.8$ center, and $\gamma = 2.0$ bottom line. The blue balls are the computed values of α with either $\alpha \equiv 0.14868 \sim \alpha_2 = \arctan(0.15) = 0.14889$ (top), $\alpha \equiv 0.3804 \sim \alpha_2 = \arctan(0.4) = 0.380506$ (center) and $\alpha \equiv 0.7852 \sim \alpha_2 = \arctan(1) = 0.785398$ (bottom) as predicted by Cor. 1 (i). In cyan the computed stress tensor τ. The deformation u is rendered in red, extremely close to $\overline{u}(x) = \gamma\, x$ rendered in green. The blue line is the rescaled deformation $u_{\text{scale}} := \gamma\, x + N(u(x) - \gamma\, x)$.

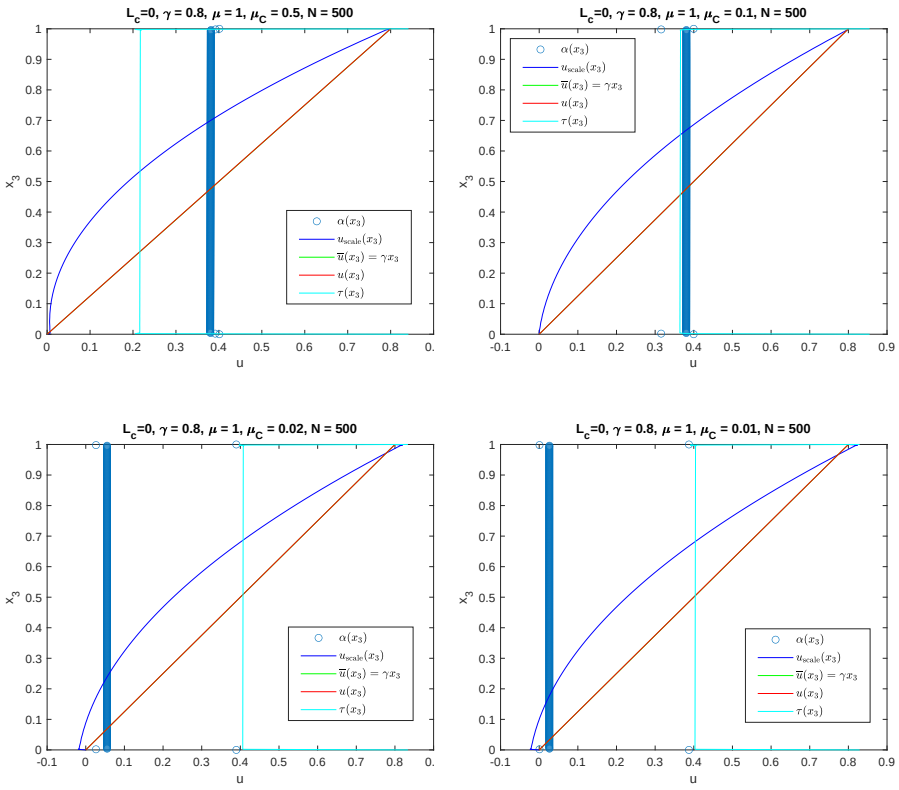


Figure 12: Minimizers of E in $\mathcal{X}^C$ for $\mu = 1$, $\gamma = 0.8$ and $N = 500$. Top left: $\mu_c = 0.5$ with $\alpha \equiv 0.3801 \approx \alpha_2 = \arctan(\gamma/2)$. Top right: $\mu_c = 0.1$ with $\alpha \equiv 0.3804 \approx \alpha_2$. Bottom left: $\mu_c = 0.02$ with $\alpha \equiv 0.0548 \approx \alpha_1^-$. Bottom right: $\mu_c = 0.01$ with $\alpha \equiv 0.026 \approx \alpha_1^-$. The results underline the validity of Cor. 1 (iii) and demonstrate that the value of μ_c selects either $\alpha_1^\pm$ or α_2 as local minimizer of $E(\overline{u}, \cdot)$, cf. Remark 7. The critical value of μ_c predicted by (56) is $\mu_c^{\text{crit}} \approx 0.0715$. In cyan the computed stress tensor τ. The deformation u is rendered in red, extremely close to $\overline{u}(x) = \gamma\, x$ rendered in green. The blue line is the rescaled deformation $u_{\text{scale}} := \gamma\, x + N(u(x) - \gamma\, x)$.

References

[1] Acerbi, E., Fusco, N. (1984). Semicontinuity problems in the calculus of variations, Archive for Rational Mechanics and Analysis 86, 125–145

[2] Appell, P. (1893). Traité de mécanique rationnelle: Statique. Dynamique du point (Vol. 1). Gauthier-Villars.

[3] Birtea, P., Caşu, I., Comănescu, D. (2020). Characterization of the critical points for the shear-stretch strain energy of a Cosserat problem. Zeitschrift für Angewandte Mathematik und Physik, 71(2), 1-17.

[4] Birsan, M., Neff, P. (2016). On the dislocation density tensor in the Cosserat theory of elastic shells, Advanced Methods of Continuum Mechanics for Materials and Structures, Advances Structures Materials, 60, K. Naumenko and M. Assmus (editors), Springer, 391–413.

[5] Blesgen, T. (2013). Deformation patterning in Cosserat plasticity, Modelling and Simulation in Materials Science and Engineering, 21(3), 35001–35012.

[6] Blesgen,T. (2014). Deformation patterning in three-dimensional large-strain Cosserat plasticity, Mechanics Research Communications (62), 37–43

[7] Blesgen, T. (2017). A variational model for dynamic recrystallization based on Cosserat plasticity, Composites B 115, 236–243

[8] Blesgen, T., Amendola, A. (2020). Mathematical analysis of a solution method for finite-strain holonomic plasticity of Cosserat materials, Meccanica 55, 621–636

[9] Borisov, L., Fischle, A., and Neff, P. (2019). Optimality of the relaxed polar factors by a characterization of the set of real square roots of real symmetric matrices. Zeitschrift für Angewandte Mathematik und Mechanik, 99(6), e201800120.

[10] Broyden, C.G. (1970). The convergence of a class of double-rank minimization algorithms, Journal of the Institute of Mathematics and its Applications. 6, 76–90

[11] Capriz, G. (1989). Continua with Microstructure. Springer.

[12] Cosserat, E., Cosserat, F. (1909). Théorie des corps déformables. Appell, Paul. Gauthier-Villars, Paris.

[13] Cosserat, E., Cosserat, F. (1991). Note sur la théorie de l'action euclidienne. Appendix in [2], 557–629.

[14] Dacorogna, B. (2008). Direct Methods in the Calculus of Variations, 2nd Edition, Springer, Berlin (2008)

[15] d'Agostino, M. V., Rizzi, G., Khan, H., Lewintan, P., Madeo, A., Neff, P. (2021). The consistent coupling boundary condition for the classical micromorphic model: existence, uniqueness and interpretation of parameters. arXiv preprint arXiv:2112.12050.

[16] Dmitrieva, O., Dondl, P. W., Müller, S., Raabe, D. (2009). Lamination microstructure in shear deformed copper single crystals. Acta Materialia, 57(12), 3439–3449.

[17] Fischle, A., Neff, P., (2017). The geometrically nonlinear Cosserat micropolar shear-stretch energy. Part I: A general parameter reduction formula and energy-minimizing microrotations in 2D, Zeitschrift für Angewandte Mathematik und Mechanik 97(7), 843–871.

[18] Fischle, A., Neff, P., Raabe, D. (2017). The relaxed-polar mechanism of locally optimal Cosserat rotations for an idealized nanoindentation and comparison with 3D-EBSD experiments. Zeitschrift für Angewandte Mathematik und Physik, 68(4), 1–30.

[19] Gastel, A. (2019). Regularity issues for Cosserat continua and p-harmonic maps. SIAM Journal on Mathematical Analysis. Vol. 51(6),4287–4310.

[20] Giaquinta, M., Hildebrandt, S. (2004). Calculus of Variations I, Springer Berlin Heidelberg

[21] Lankeit, J., Neff, P., Osterbrink, F. (2017). Integrability conditions between the first and second Cosserat deformation tensor in geometrically nonlinear micropolar models and existence of minimizers. Zeitschrift für Angewandte Mathematik und Physik Vol. 68(1), 1–19.

[22] Li, Y., Wang, C. (2022). Regularity of weak solution of variational problems modeling the Cosserat micropolar elasticity. International Mathematics Research Notices. Vol. 2022(6). Oxford University Press, 4620–4658.

[23] Mariano, P. M., Modica, G. (2009). Ground states in complex bodies. ESAIM: Control, Optimisation and Calculus of Variations, 15(2), 377–402.

[24] Müller, S. (1998). Variational models for microstructure and phase transitions, Lecture Notes no. 2, Max-Planck-Institute for Mathematics.
https://www.mis.mpg.de/publications/other-series/ln/lecturenote-0298.html

[25] Neff, P. (2004). Existence of minimizers for a geometrically exact Cosserat solid. Proceedings in Applied Mathematics and Mechanics, 4(1). Wiley Online Library, 548–549.

[26] Neff, P., Bîrsan, M., Osterbrink, F. (2015). Existence theorem for geometrically nonlinear Cosserat micropolar model under uniform convexity requirements. Journal of Elasticity, 121(1), 119–141.

[27] Neff, P., Lankeit, J., Madeo, A. (2014). On Grioli's minimum property and its relation to Cauchy's polar decomposition. International Journal of Engineering Science. 80, 209–217.

[28] Neff, P., Fischle, A. and Borisov, L. (2019). Explicit global minimization of the symmetrized Euclidean distance by a characterization of real matrices with symmetric square. SIAM Journal on Applied Algebra and Geometry. 3(1). 31–43.

[29] Neff, P., Fischle, A., Münch, I.(2008). Symmetric Cauchy stresses do not imply symmetric Biot strains in weak formulations of isotropic hyperelasticity with rotational degrees of freedom. Acta Mechanica. 197(1), 19–30.

[30] Neff, P., Münch, I. (2008). Curl bounds Grad on SO(3). ESAIM: Control, Optimisation and Calculus of Variations 14(1), 148–159.

[31] Neff, P., Münch, I. (2009). Simple shear in nonlinear Cosserat elasticity: bifurcation and induced microstructure. Continuum Mechanics and Thermodynamics, 21(3), 195–221.

[32] Struwe, M. (2008). Variational Methods: Applications to Nonlinear Partial Differential Equations and Hamiltonian Systems, 4th Edition, Springer, Berlin (2008).